JPRS L/10463

15 April 1982

Translation

OPTICAL METHODS FOR PROCESSING IMAGES AND SIGNALS

Ed. by

V.A. Potekhin

FBIS FOREIGN BROADCAST INFORMATION SERVICE

FOR OFFICIAL USE ONLY

APPROVED FOR RELEASE: 2007/02/09: CIA-RDP82-00850R000500050039-9

NOTE

JPRS publications contain information primarily from foreign newspapers, periodicals and books, but also from news agency transmissions and broadcasts. Materials from foreign-language sources are translated; those from English-language sources are transcribed or reprinted, with the original phrasing and other characteristics retained.

Headlines, editorial reports, and material enclosed in brackets [] are supplied by JPRS. Processing indicators such as [Text] or [Excerpt] in the first line of each item, or following the last line of a brief, indicate how the original information was processed. Where no processing indicator is given, the information was summarized or extracted.

Unfamiliar names rendered phonetically or transliterated are enclosed in parentheses. Words or names preceded by a question mark and enclosed in parentheses were not clear in the original but have been supplied as appropriate in context. Other unattributed parenthetical notes within the body of an item originate with the source. Times within items are as given by source.

The contents of this publication in no way represent the policies, views or attitudes of the U.S. Government.

APPROVED FOR RELEASE: 2007/02/09: CIA-RDP82-00850R000500050039-9

JPRS L/10463

15 April 1982

OPTICAL METHODS FOR PROCESSING IMAGES AND SIGNALS

Leningrad OPTICHESKIYE METODY OBRABOTKI IZOBRAZHENIY I SIGNALOV in Russian 1981 (signed to press 10 Jun 81) pp 1-101

[Collection "Optical Methods for Processing Images and Signals," edited by Doctor of Technical Sciences Professor V. A. Potekhin, Physico-technical Institute imeni A. F. Ioffe, USSR Academy of Sciences, 500 copies, 101 pages]

CONTENTS

[Text] This collection contains individual reports delivered and discussed at meetings of the section on non-optical holography at the Leningrad Regional Board of the S. I. Vavilov Scientific and Technical Society of the Instrument Making Industry. The section was organized in 1977 at the initiative of the directorate of the section on holography at the Central Board of the S. I. Vavilov Scientific and Technical Society of the Instrument Making Industry. This section now brings together Leningrad scientists and engineers from institutions of higher education and research institutes working in the fields of applied use of methods of radio and acoustic holography, as well as optical processing of radio and acoustic signals. The articles mainly give the results of original research by the authors dealing with current problems of using methods of holography and optical processing of information in microwave engineering.

The Science Council on the Problem of Holography Affiliated With the Presidium of the USSR Academy of Sciences was of considerable assistance in organizing and publishing this collection. The directorate of the section on non-optical holography is sincerely grateful to Doctor of Physical and Mathematical Sciences S. B. Gurevich, and Candidate of Physical and Mathematical Sciences G. A. Gavrilov for expediting publication of the collection, and also to Associate Member of the USSR Academy of Sciences L. D. Bakhrakh for reading the manuscript. The directorate of the section thanks the authors who delivered these papers, and who offered them for publication in this collection.

UDC 778.4:523.164.8

USING HOLOGRAPHIC PRINCIPLES TO ANALYZE RADAR STATIONS WITH SYNTHESIZED APERTURE

[Article by Yu. S. Zinov'yev and A. Ya. Pasmurov]

[Text] An examination is made of major aspects of holographic theory of radar with synthesized aperture [RSA]. The first stage of holographic processes in RSA (formation of radio

hologram) is treated as recording of the field scattered by an object by using an artificial reference source. The second stage (reconstructing the object) is described on the basis of physical optics. A classification is given of radio holograms recorded in the RSA and conditions of subsequent processing. A physical interpretation is given of major RSA parameters. An examination is made of application of the proposed theory to evaluating the influence of trajectory instabilities of the RSA carrier, and to analyzing images of moving observational objects.

1. Introduction

Up until the present, the description of RSA has used mainly such methods as the synthesized antenna technique, the method of signal selection by Doppler frequencies, the method of cross correlation, which are based on principles of the theory of electronic systems, optimum reception theory and the like. All three approaches enable evaluation of the influence that technical parameters of the RSA have on its tactical characteristics [Ref. 1, 2]. Results and conclusions practically coincide.

The RSA in combination with a coherent optical processor [Ref. 3] is a "quasi-holographic" system in which resolution with respect to one coordinate (azimuth) is attained by holographic processing of a fixed signal. In the opinion of Leith and Ingalls [Ref. 4] such a representation is the most flexible and physically graphic and enables development of RSA components with working principle that is readily explained by the theory of radio systems. This viewpoint has been developed by Kock [Ref. 5], with proposal of some new radar systems based on principles of holograms. However, the use of the holographic approach for analyzing the RSA has been limited until now to examination of only optical processors. There is practically no mathematically valid viewpoint enabling representation of the RSA as a whole as a holographic system. Therefore description of the RSA from unified holographic principles is of theoretical interest. Such an analysis gives the most complete elucidation of the essence of physical processes that take place in the RSA. In addition, it becomes possible to use concepts and methods developed in the theory of optical holography.

2. Principles of obtaining holograms in RSA

Let us consider an RSA (Fig. 1) mounted on a vehicle moving at velocity v_H along axis x'. The radar antenna has linear dimension L_R (real aperture), and width of radiation pattern θ_R along the line of the path. The radar scans a strip in short pulses and fixes the pattern of diffraction of the probing signal by the observational objects sequentially in time. The amplitude and phase of the scattered field are registered by interference of received and reference

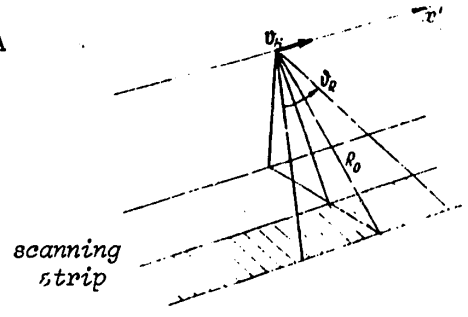

Fig. 1. Principal geometric relations in RSA

signals in a coherent (synchronous) detector. As a result, a radio hologram of multiplicative type is formed [Ref. 6], the part of the reference wave being played by a signal introduced directly into the electronic channel ("artificial" reference wave). The radio hologram is usually recorded by modulation of CRT luminescence intensity on a photographic film moving relative to the CRT screen at velocity v_n. To record radio holograms of objects situated at different ranges R_0 from the line of the path, the pulsed mode of operation is used with vertical scanning on the CRT screen. The result is a set of one-dimenisonal holograms recorded in different positions with respect to the width of the film, depending on the range to the corresponding objects.

Let us assume that all objects are located at a distance R_0 from the line of the path. In this case the radiated signal can be considered continuous since accounting for the pulsed nature of the radiation is important only for analyzing the resolution of objects with respect to range. Fig. 2 shows the equivalent diagram of recording a one-dimensional radio hologram. Situated at point Q with coordinates (x', 0) is an RSA ($x' = v_H t$, where t is elapsed time), and at point R (x_r, z_r) is a hypothetical reference wave source with action similar to that of a reference signal of the synchronous detector, while point P (x_0, $z_0 = -R_0$) belongs to the observed object situated along axis x_0. If the scattering properties of the object are described by the function $F(x_0)$, and dimensions are sufficiently small compared to the quantity R_0, we get the well known Fresnel approximation [Ref. 7] for the diffraction field along axis x' (with consideration of propagation of the probing signal from the RSA to the object and back)

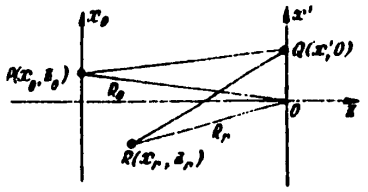

Fig. 2. Equivalent diagram of recording one-dimensional hologram

$$U_0(x') = C \frac{e^{i\kappa_1 R_0}}{\sqrt{\lambda_1 R_0}} \int_{-\infty}^{\infty} F(x_0) e^{i\kappa_1 \frac{(x_0 - x')^2}{R_0}} dx_0 , \qquad (1)$$

where $\kappa_1 = 2\pi/\lambda_1$ is the wave number, and C stands for some complex constant both here and below.

The complex amplitude of the reference wave is $U_r(x') = A_r e^{i\phi_r}$. Usually this is a plane wave, i. e. $\phi_r = \kappa_1 \sin\theta x'$, where θ is the angle of "incidence" of the wave on the hologram. The inclination of the reference wave is equivalent to a reference signal with linear phase advance, and introduces carrier frequency $\omega_x = \kappa_1 \sin\theta$. As a result of coherent detection, we get a radio hologram with equation

$$h(x') = \mathrm{Re}(U_r^*(x') U_0(x')) \quad \text{or} \quad h(x') = \mathrm{Im}(U_r^*(x') U_0(x')) . \qquad (2)$$

With consideration of (1), it is clear that in the general case one-dimensional Fresnel radio holograms are formed in the RSA. In addition, the following situations are possible, depending on the ratio of dimensions of

the object, the length of the synthesized aperture $L_s = v_H T$ (T is the time of recording the radio hologram) and the quantity R_0.

1. In the case where $R_0 >> \kappa_1 x_{0max}^2/2$ (x_{0max} is a quantity that characterizes the maximum dimensions of the object), instead of (1) we get the Fraunhofer approximation

$$U_0(x') = C \frac{e^{i\kappa_1 R_0}}{\sqrt{\lambda_1 R_0}} e^{\frac{i\kappa_1 x'^2}{R_0}} \int_{-\infty}^{\infty} F(x_0) e^{-i\kappa_1 \frac{2x'x_0}{R_0}} dx_0 , \quad (3)$$

and as a result a Fraunhofer radio hologram is formed.

2. In the case where $R_0 >> \kappa_1 x_{max}/2 = \kappa_1 L_s^2/8$, the term $e^{j\kappa_1 x'^2/R_0}$ in (3) can be omitted. Then a Fourier radio hologram is formed, and the condition of formation in the RSA can be written as

$$L_s \leq \rho \sqrt{\lambda_1 R_0/\pi} . \quad (4)$$

3. If the object is a point ($F(x_0) \sim \delta(x' - x_0)$), the Fraunhofer diffraction conditions are automatically satisfied. Using the filtering properties of the δ-function, expression (3) yields the following equation of the radio hologram (without consideration of constant phase terms)

$$h(x') = A_r A_0 \cos(\omega_r x' - \kappa_1 \frac{x'^2}{R_0} + 2\kappa_1 \frac{x'x_0}{R_0}) , \quad (5)$$

where A_0 is the amplitude of the wave scattered by the object at the reception point.

If in addition (4) is valid, then (5) implies

$$h(x') = A_r A_0 \cos(\omega_c x' + 2\kappa_1 \frac{x'x_0}{R_0}) . \quad (6)$$

Thus a Fraunhofer or Fourier radio hologram is formed in the RSA for a point target. In the former case the radio hologram has the form of a one-dimensional Fresnel zone plate in accordance with (5), and in the latter case it takes the form of a one-dimensional diffraction grating with constant spacing in accordance with (6).

In the process of photographic recording, scaling of the radio holograms takes place with substitution of coordinate x for x', where $x = x'/n_x$, and $n_x = v_H/v_n$. In this operation, a constant term h_0 ("displacement") is added to (5) and (6) for photographic recording of the function h(x').

3. Image Reconstruction

We will analyze the next stage of the holographic process by the method of physical optics. Illuminating a phototransparency by a plane wave with wave number κ_2, we get a diffraction field with distribution at distance ρ from

the hologram described by the Huygens-Fresnel integral

$$V(\xi) = \frac{e^{i(\kappa_2\rho - \pi/4)}}{\sqrt{\lambda_2 \rho}} \int_{-U_0T/2}^{U_0T/2} h(x) e^{i\frac{\kappa_2}{2\rho}(x-\xi)^2} dx \,. \tag{7}$$

Substituting (6) in (7) we have $V(\xi) = V_0(\xi) + V_1(\xi) + V_2(\xi)$, where $V_0(\xi)$ is the zero order corresponding to displacement h_0, $V_1(\xi)$ and $V_2(\xi)$ are functions that describe the reconstructed images of the point object and are equal to

$$\left.\begin{matrix} V_1(\xi) \\ V_2(\xi) \end{matrix}\right\} = C \int_{-U_0T/2}^{U_0T/2} e^{i\left(\frac{\kappa_2}{2\rho} \pm \frac{\kappa_1 n_x^2}{R_0}\right)x^2} e^{-i\left[\frac{\kappa_2 \xi}{\rho} \mp (\omega_x n_x + \frac{2\kappa_1 n_x x_0}{R_0})\right]x} dx \,. \tag{8}$$

We find the position of the images along the z-axis from the condition of a zero value of the exponent in the first exponential function of (8), implying

$$\rho = \pm \lambda_1 R_0 / 2\lambda_2 n_x^2 \,. \tag{9}$$

Obviously one image is imaginary and the other is real. Integrating (8) with condition (9) we get

$$\left.\begin{matrix} V_1(\xi) \\ V_2(\xi) \end{matrix}\right\} = C \frac{\sin\left[(\omega_x n_x + \frac{2\kappa_1 n_x^2}{R_0}(\frac{x_0}{n_x} - \xi)\right]\frac{U_0T}{2}}{\left[\omega_x n_x + \frac{2\kappa_1 n_x^2}{R_0}(\frac{x_0}{n_x} - \xi)\right]\frac{U_0T}{2}} \tag{10}$$

Thus the image of a point object is described by a function of type $\sin\nu/\nu$. The position of the image is determined by the zero value of the argument ν, i. e. by the relation

$$\xi = x_0/n_x + \omega_x R_0 / 2\kappa_1 n_x \,. \tag{11}$$

The first term in (11) corresponds to the coordinate of the object, and the second term is due to the carrier frequency. The images of two point objects that have identical coordinates x_0 but different ranges R_1 and R_2 will be characterized by different coordinates ξ_1 and ξ_2. Thus the use of a carrier frequency leads to geometric distortions of the image of the entire scanning strip.

According to the Rayleigh criterion, two points are considered as separate if the principal maximum of one of the functions of the type $\sin\nu/\nu$ coincides with the first zero of the second function. From this we get an estimate of the resolution

$$\Delta x' = x_1 - x_2 = \pi R_0 / \kappa_1 L_x \,. \tag{12}$$

The given case (use of Fraunhofer radio holograms) has been called the "focused aperture" in RSA theory. Focusing is understood as compensation of the quadratic phase advance in equation (5) on the stage of image reconstruction (compensation is accomplished by transformation (7)).

The case of the "unfocused aperture" corresponds to the equation of the Fourier radio hologram (6). Therefore, Fourier transformation of the function of the radio hologram is used on the processing stage

$$V(\xi_0) = C\int_{-v_0T/2}^{v_0T/2} h(x)e^{-i\kappa_2 x\xi/\rho}\,dx \quad . \tag{13}$$

From (13) with consideration of (6) we get

$$\left.\begin{matrix}V_1(\xi)\\ V_2(\xi)\end{matrix}\right\} = C\,\frac{\sin\left\{\left[\frac{\kappa_2}{\rho}\xi \pm (\omega_x n_x + \frac{2\kappa_1}{R_0} n_x x_0)\right]\frac{v_0 T}{2}\right\}}{\left[\frac{\kappa_2}{\rho}\xi \pm (\omega_x n_x + \frac{2\kappa_1}{R_0} n_x x_0)\right]\frac{v_0 T}{2}} \quad . \tag{14}$$

In the given case the quantity ρ can be treated as the focal length of the Fourier lens. The position of the image of the point object is determined by the equation

$$\xi = \pm\frac{\rho}{\kappa_2}(\omega_x n_x + \frac{2\kappa_1}{R_0} n_x x_0) \quad . \tag{15}$$

The image of the entire scanning strip will also be distorted as a consequence of the dependence of ξ on range R_0. Evaluation of the resolution according to the Rayleigh criterion gives

$$\Delta x' = x_1 - x_2 = \pi R_0/\kappa_1 n_x v_0 T \quad . \tag{16}$$

The limiting attainable resolution in an RSA with unfocused processing with consideration of (4) is

$$\Delta x' = \sqrt{\pi\lambda_1 R_0}/4 \approx 0{,}44\sqrt{\lambda_1 R_0} \quad . \tag{17}$$

It should be noted that radio holograms are recorded continuously on photographic film in the course of a prolonged flight. Therefore the focused or unfocused mode is assigned only on the stage of reconstructing the image by selecting the dimensions of the diaphragm that determines the quantity L_s/n_x, and through corresponding design of the optical processing arrangement.

Let us now consider the RSA from the standpoint of the geometric method developed in Ref. 8, 9 and assuming analysis of the phase structure of the radio hologram. For this purpose we rewrite one of the equations (2) in the form

$$h(x') = A_r A_0 \cos(\varphi_r - \varphi_0) \quad ,$$

where ϕ_0 is the phase of the wave scattered by the object.

For a point object situated at point P (Fig. 2), we can write (with consideration of wave propagation from the RSA to the object and back): $\phi_0 = 2\kappa_1(PQ - PO)$ and $\phi_r = 2\kappa_1(RQ - RO)$, where $RO = R_r$ is the distance from the hypothetical source of the reference wave to the coordinate origin. Expanding ϕ_r and ϕ_0 in a

series and limiting ourselves to first-order terms, we get

$$\varphi_r - \varphi_0 \approx -\frac{4\pi}{\lambda_1}\left[x'^2\left(\frac{1}{2R_r} - \frac{1}{2R_0}\right) - x'\left(\frac{x_r}{R_r} - \frac{x_0}{R_0}\right)\right]. \tag{18}$$

In the simplest case where $x_0 = 0$, $x_r = 0$, $R_r = \infty$ (plane reference wave without linear phase advance), we get

$$\varphi_r - \varphi_0 = 4\pi x'^2 / 2\lambda_1 R_0 .$$

The spatial frequency of the interference pattern is

$$\nu(x') = \frac{1}{2\pi}\frac{\partial(\varphi_r - \varphi_0)}{\partial x'} = 2x'/\lambda_1 R_0 . \tag{19}$$

At some value $x'_{cr} = L_{s_{max}}/2$, the frequency ν may exceed the resolution of the field recorder, which is determined in the given case by the actual aperture of the radar set, and is equal to $\nu_{cr} = 1/L_R$. This implies the condition

$$L_{s_{max}} \leq \lambda_1 R_0 / L_R = \vartheta_R R_0 . \tag{20}$$

Substituting the value of $L_{s_{max}}$ in (12), we get the classical relation for maximum attainable resolution in the RSA:

$$\Delta x_{np} = L_R/2 .$$

Accounting for the pulsed nature of the signal enables us to determine such an important parameter of the radar set as the minimum value of the probing pulse recurrence rate κ_{min}. Obviously the pulsed mode is analogous to discretization of the radio hologram. The distance between individual readings $\Delta x' = v_H/\kappa$ must satisfy the condition $\Delta x' \leq [2\nu(x'_{cr})]^{-1}$, whence with consideration of (19) we have

$$\kappa_{min} = 2v_H/L_R .$$

Following the known procedure of Ref. 8, 9, we get relations that determine the deviation of the phase front of the reconstructed wave from spherical (third-order wave aberrations)

$$\Delta\varphi^{(3)}_m = -\frac{\kappa^2}{2}\left(D_0\frac{x^4}{4} - D_1 x^3 + D_2 x^2\right), \tag{21}$$

where

$$D_\kappa = \frac{x_c^\kappa}{R_c^3} - \frac{x_I^\kappa}{R_I^3} \pm \frac{2\mu}{m^{4-\kappa}}\left(\frac{x_0^\kappa}{R_0^3} - \frac{x_r^\kappa}{R_r^3}\right) .$$

x_c and R_c are coordinates of the source of the reconstructing wave, $\mu = \lambda_1/\lambda_2$ $m = n_x^{-1}$, and the coordinates of the image of the point object are

$$\frac{1}{R_I} = \frac{1}{R_c} \pm \frac{2\mu}{m^2}\left(\frac{1}{R_0} - \frac{1}{R_r}\right) \text{ and } \frac{x_I}{R_I} = \frac{x_c}{R_c} \pm \frac{2\mu}{m}\left(\frac{x_0}{R_0} - \frac{x_r}{R_r}\right).$$

The value $\kappa = 0$ corresponds to spherical aberration, $\kappa = 1$ to coma, and $\kappa = 2$ to astigmatism. These relations can be used to calculate the maximum permissible size of the synthesized aperture $L_{S_{max}}$ on the basis of the Rayleigh condition (wave aberrations on the edges of the hologram should not exceed $\lambda_2/4$). Considering that spherical aberrations are the most appreciable in order of magnitude, we get

$$L_{S_{max}} = 2\sqrt[4]{\lambda_1 R_0^3 / \left(1 - 4\frac{M^2}{m^2}\right)} . \qquad (22)$$

For typical conditions of RSA operation, the quantity $L_{S_{max}}$ calculated by formula (20) is less than the value calculated by formula (22), i. e. the influence of wave aberrations in the RSA is insignificant.

4. Influence of RSA Trajectory Instabilities

Instability of the vehicle trajectory is one of the major factors that distort the images obtained by the RSA. The holographic treatment enables fairly simple evaluation of permissible deviations of the trajectory from linear by the method of geometric optics. Let us write the expression for the phase of the object wave $\phi_0(x')$ in the form

$$\varphi_0(x') = -2\kappa_1 \left\{ \left[(z_0 - q)^2 + (x' - x_0)^2 \right]^{1/2} - R_0 \right\} ,$$

where $q = q(x')$ is displacement of the trajectory from the x'-axis.

Assuming that $R_0 >> x_0$, x' and q, using the binomial expansion and dropping all terms of the order of q^2 and higher, we get the following approximate expression for $\phi_0(x')$:

$$\varphi_0(x') \cong -\frac{4\pi}{\lambda_1}\left(\frac{x'^2 - 2x_0 x'}{2R_0} - \frac{x^4 - 4x_0 x'^3 + 4x_0^2 x'^2}{8R_0^3} - \frac{z_0 q}{R_0} + \frac{z_0 q x'^2 - 2z_0 q x_0 x'}{2R_0^3} \right).$$

The equation for the phase of the wave that forms one of the reconstructed images has the usual form

$$\varphi_1 = \varphi_c \pm (\varphi_0 - \varphi_r) . \qquad (23)$$

On the other hand, the function ϕ_1 can be written as

$$\varphi_1 = -\frac{2\pi}{\lambda_2}\left(\frac{x^2 - 2x_1 x}{2R_1} - \frac{x^4 - 4x_1 x^3 + 4x_1^2 x^2}{8R_1^3} \right) . \qquad (24)$$

The phases ϕ_c and ϕ_r are determined by expressions analogous to (24). The differences between phases of corresponding third-order terms relative to $1/R_1$ in (23) and (24) are aberrations equal to

$$\Delta\Phi = \Delta\varphi^{(3)} + \Delta\varphi^{(3)}_{true}$$

Aberrations $\Delta\phi^{(3)}$ are determined by expression (21), and

$$\Delta\varphi^{(3)}_{\text{true}} = -\kappa_2(D_3\vartheta + D_4\vartheta x - D_5\vartheta x^2), \tag{25}$$

where

$$D_3 = \mp 2\mu z_0/R_0, \quad D_4 = \mp 2\mu z_0 x_0/mR_0^3, \quad D_5 = \mp \mu z_0/m^2R_0^3$$

are aberrations due to trajectory instabilities.

Relation (25) that determines the distortions of the phase structure of the radio hologram can be used for calculating the compensating phase shift directly in the process of synthesis. To do this, it is advisable to use digital methods of signal processing in the RSA.

Applying the Rayleigh criterion to each of the terms in (25), we get the following conditions for permissible deviations of the vehicle trajectory:

$$\vartheta_3 \le \lambda_2/4\cdot|D_3| = \lambda_1 R_0/8z_0 = \lambda_1/8\cos\theta_0, \tag{26}$$

$$\vartheta_4 \le \lambda_2/4\cdot|D_4|_{x\max} = \lambda_1 R_0^3/4L_S z_0 x_0, \tag{27}$$

$$\vartheta_5 \le \lambda_2/4\cdot|D_5|_{x^2_{\max}} = \lambda_1 R_0^3/z_0 L_S^2. \tag{28}$$

On the other hand, knowing flight conditions and the characteristics of the vehicle, we can use (26)-(28) to determine the limitations imposed on the quantity $\cos\theta_0$ and the limiting permissible dimension of the synthesized aperture:

$$\cos\theta_0 \le \lambda_1/8\vartheta, \quad L_{S\max} \le \lambda_1 R_0^2/4\vartheta x_0, \quad L_{S\max} < R_0\sqrt{\lambda_1/\vartheta}.$$

As a rule, the relations $L_S \ll R_0$ and $x_0 \ll R_0$ are satisfied in the RSA. Therefore the quantities D_4 and D_5 can be disregarded, with account taken only of the factor D_3 which according to (26) imposes severe conditions on the stability of the trajectory.

5. Influence of Motion of the Object of Observation

The effects that arise in the RSA when observing moving objects can be evaluated from the standpoint of the method of physical optics. Let a point object move at low velocity v_0 in the radial direction (along the z-axis), so that for the time of synthesis T the displacement of the object does not exceed the resolution with respect to range. In this case, the equation of the radio hologram takes the form (disregarding constant phase terms):

$$h(x)\sim\cos\left(\omega_x\eta_x x + 2\kappa_1\frac{v_0}{v_H}\eta_x x - \kappa_1\frac{\eta_x^2 x^2}{R_0} + 2\kappa_1\frac{\eta_x x_0 x}{R_0} - \frac{\kappa_1}{R_0}\left(\frac{v_0}{v_H}\right)^2\eta_x^2 x^2\right). \tag{29}$$

Substituting (29) in (7), we get the following condition of observation of a focused image:

$$\rho = \pm\left(\frac{\kappa_2}{2\kappa_1}\cdot\frac{R_0}{\eta_x^2}\right)\Big/\left[1+\left(\frac{v_0}{v_H}\right)^2\right].$$

Since the quantity $v_0/v_H \ll 1$, the image will be observed practically in the same plane as for a stationary object. Considering this fact, and carrying out the integration, we get a function that describes one of the reconstructed images:

$$V(\xi) = C \frac{\sin\left\{\left[\omega_1 n_x + 2K_1 \frac{v_0}{v_H} n_x + \frac{2K_1 n_x}{R_0}(x_0 - n_x \xi)\right] \frac{v_H T}{2}\right\}}{\left[\omega_1 n_x + 2K_1 \frac{v_0}{v_H} n_x + \frac{2K_1 n_x}{R_0}(x_0 - n_x \xi)\right] \frac{v_H T}{2}}$$

The position of the image is determined by the equation

$$\xi = \frac{x_0}{n_x} + \frac{\omega_1 R_0}{2K_1 n_x} + \frac{R_0}{n_x} \cdot \frac{v_0}{v_H} .$$

Obviously motion of the object is equivalent to introducing an additional carrier frequency on the stage of recording the radio hologram, and it leads to displacement of the image. The optical processor uses the real image that is recorded on photographic film. The field of view on this film is limited by a diaphragm that cuts off background illumination. The quantity v_0 may reach a value such that the image of the object will not be registered at all because of the shift.

Motion of the object in the azimuthal direction (along the x'-axis) with velocity v_0 is equivalent to a change in the flight velocity of the vehicle. In this case, relation (9) that determines the position of the focused image along the z-axis can be rewritten as

$$\rho' = \pm \lambda_1 R_0 / 2\lambda_2 n_x^2 = \pm \lambda_1 R_0 v_H^2 / 2\lambda_2 (v_H - v_0)^2 .$$

Thus motion of the object along the x'-axis leads to a change in conditions of focusing by the quantity

$$\delta\rho = \rho' - \rho = 2\rho \frac{v_0}{v_H}\left(1 - \frac{v_0}{2v_H}\right) \Big/ \left(1 - \frac{v_0}{v_H}\right)^2 , \qquad (30)$$

where ρ is defined by expression (9).

If $v_0 \ll v_H$, then

$$\delta\rho \approx 2\rho v_0 / v_H . \qquad (31)$$

From equation (30) we can get

$$v_0 = v_H\left(1 - \sqrt{1 - \delta\rho/(\rho + \delta\rho)}\right) .$$

On the other hand, from the simplest geometric considerations we find the following expression for resolution of the RSA along the z-axis (longitudinal resolution):

$$\Delta\rho = 2(\Delta x' v_0)^2 / \lambda_2 v_H^2 \approx 2(\Delta x')^2 / \lambda_2 n_x^2 . \qquad (32)$$

The depth of focusing $\Delta\rho$ is defined as displacement from the focal plane along the z-axis by a distance for which the azimuthal resolution $\Delta x'$ detrriorates to half as compared with the diffraction limit (12).

To observe a focused image of an object moving at velocity v_0, additional focusing of the optical processor is necessary. The velocities of the object at which focusing is necessary we get from the condition $\Delta\rho < \delta\rho$, where $\delta\rho$ is assigned by (31). Using (9) and (32), we get

$$v_0 > R(\Delta x')^2 v_н / \lambda_1 R_0 \quad .$$

At lower velocities of motion of the object, refocusing of the processor is not required, and deterioration of image quality can be considered insignificant.

6. Conclusion

To describe the working principles of the RSA, in addition to known methods [Ref. 1, 2] that have been extensively used heretofore, a holographic approach can be used that represents the RSA and the optical processor as an integral unit. The given examples confirm the physical clarity and fruitfulness of the proposed approach for analyzing the RSA.

REFERENCES

1. Reutov, A. P., Mikhaylov, B. A., Kondratenkov, G. S., Boyko, B. V., "Radiolokatsionnyye stantsii bokovogo obzora" [Side-Looking Radar], Moscow, "Sov. radio", 1970.

2. R. O. Harger, "Synthetic Aperture Radar Systems, Theory and Design", Ac. Press, N. Y., 1970, pp 18-58.

3. Leith, TIIER, Vol 59, No 9, 1971, pp 25-44.

4. Leith, E., Ingalls, M., APPL. OPTICS, Vol 7, No 3, 1968, pp 539-544.

5. Kock, W. E., "Recent Developments ir Holography", PROGR. ELECTRO-OPT., REV. RECENT DEV., 1975, pp 45-66.

6. Popov, S. A., Rozanov, B. A., Zinov'yev, Yu. S., Pasmurov, A. Ya., "Sb. Materialy VIII Vsesoyuznoy shkoly po golografii" [Collected Materials of the Eighth All-Union School on Holography], Leningrad, 1976, pp 275-286.

7. A. Papulis, "Teoriya sistem i preobrazovaniy v optike" [Theory of Systems and Transformations in Optics], Moscow, "Mir", 1971.

8. Meier, R. W., JOSA, Vol 55, No 7, 1965, pp 987-991.

9. Champagne, E. B., JOSA, Vol 57, No 1, 1967, pp 51-55.

UDC 621.391.266

EQUAL OBSERVATION PRINCIPLE AND ECONOMIC ALGORITHMS FOR SIGNAL PROCESSING IN QUASI-HOLOGRAPHIC PULSE-DOPPLER SYSTEMS

[Article by B. S. Mush]

[Text] An equation is given that relates the signal of a quasi-holographic pulse-Doppler system to a function that describes reflective surface properties. This is called the principal equation. An equal observation principle is introduced that minimizes uncertainty in evaluating the reflective surface function that arises in solving the principal equation. Algorithms are considered for solving the principal equation by a direct method and by the method of fast Fourier transforms to calculate correlation sums, and the efficiency of these algorithms is evaluated with respect to a criterion of the minimum number of operations per unit area of the surface being evaluated with consideration of the equal observation principle. It is shown that there is an optimum ratio of sides of the correlation matrix.

The concept of the quasi-holographic pulse-Doppler system was qualitatively introduced in Ref. 1. The signal S(t) at its input can be represented as an integral equation of the first kind with a difference kernel and unknown reflective surface function:

$$\iint_{L_{ox}L_{oy}} K_x(X(t)-x)K(Y'(t)-y)f(x,y)\,dx\,dy = S_3(t)\cdot\exp 2ikt,$$

$$S(t) = S_3(t)\cdot J(Y(t), Z(t)),$$

$k = \frac{2\pi}{\lambda}$, λ is the wavelength of the system,

$$K_x(v) = G_x^2\left(\frac{v}{Y(t)}\right)\cdot\exp -ik\frac{v^2}{Y(t)},$$

$$K_y(v) = Q(v)\cdot\exp 2ikv,$$

$$Y'(t) = Y(t) + \frac{ct}{2},$$

$$J(Y,Z) = \frac{4\pi}{Y^2}\cdot G_z^2\left(\frac{Z}{Y}\right)\cdot\exp ik\frac{Z^2}{Y},$$

Q(t) is a complex function that characterizes the shape of the emitted signal; X(t), Y(t), Z(t) are the projections of the radius-vector of the phase center of the antenna on the x, y, z axes of the coordinate system fixed to the surface on which the region [L_{ox}, L_{oy}] of definition of f(x,y) is assigned, the y-axis being collinear with the ray corresponding to the maximum of the antenna radiation pattern G(x,y,z), and

$$G(x,y,z) = G_x\left(\frac{x-X}{Y}\right)\cdot G_z\left(\frac{Z}{Y}\right).$$

The initial equation, which will hereafter be called the principal equation, can be represented as a system of two homogeneous difference equations:

$$\int_{L_y} K_y(y'(t)-y)\cdot\bar{f}_y(y,t)\,dy = s_y(t),$$
$$\int_{L_x} K_x(X(t)-x)\cdot f(x,y)\,dx = \bar{f}_y(y,t).$$

Systematic solution of this equation leads to finding the reflective surface function — a procedure corresponding to the main job of the radio-holographic system.

To analyze the problem of synthesizing economic algorithms for solving the principal equation, it is sufficient to consider a procedure for solving either of the equations of this system. To be specific, our further analysis will apply to the first equation, and we will omit the subscript y in denoting the interval of evaluation of the reflective surface function.

In actual systems, the signal is measured on the finite interval L_T over which the estimate of the reflective surface function is defined on some interval L_O. If the interval of surface coverage L_G is commensurate with L_T, then a contradictory situation must be considered: either the reflective surface function is evaluated from signals generated by a reflective surface function with region of definition much greater than L_O, or the time of observation of elements of the reflective surface function on interval L_O is inconstant. Both factors cause uncertainty in estimating reflective surface functions when solving the principal equation. In connection with the given signal formation property due to the structure of the kernel of the principal equation, we formulate the equal observation principle: when solving the principal equation with respect to signals assigned on a fixed interval of observation L_T, the intervals of estimation of the reflective surface function L_O must be selected such that all its infinitesimal elements are observed for an equal time.

Calculation of the estimate $\hat{f}$ of the reflective surface function by means of the kernel R of the inverse transform causes considerable difficulties that are associated with the necessity of carrying out a large number of arithmetic operations for computing correlation sums of the form

$$\hat{f}_k = \sum_{n=0}^{N-1} R(k-n)\cdot s_n, \quad k = 0,1,\ldots,P-1, \tag{1}$$

where $\hat{f}_K$ and S_n are discrete readings of the functions $\hat{f}(x)$ and $S(X)$.

In the direct method of calculating $\hat{f}_K$, 2NP multiplications and additions must be carried out. Use of the method of generalized Fourier transforms enables us to apply effective fast Fourier transform methods [Ref. 2]. Let us consider estimates of $\hat{f}_K$ obtained by the method of fast Fourier transforms.

Let $P \leq N$. Then assuming periodicity R(n) with period N

$$\hat{f}_k = F^{-1}[\tilde{S}_j(N) \cdot \tilde{R}_j(N)],$$

where $\tilde{S}_j(N)$ and $\tilde{R}_j(N)$ are generalized Fourier transforms of S_n and R(n) on the interval $j = 0, 1, \ldots N-1$ with period N, and F^{-1} is the inverse generalized Fourier transform. In the following, we will limit ourselves to the use of fast Fourier transforms to the base 2. Then to calculate $\hat{f}_k$ it is necessary to perform $(3 \log_2 N + 2)N$ arithmetic and logic operations ($3N \log_2 N$ in calculating the fast Fourier transforms, N in multiplying spectra, and N in transposition of data).

Let $P > N$. Then the assumption of periodicity R(n) with period N is not permissible. Let us turn to a widely used method: we write sum (1) as

$$\hat{f}_k = \sum_{n=0}^{P-1} R(k-n)\,\bar{S}_n,$$

$$\bar{S}_n = \begin{cases} S_n, & \text{if } 0 \leq n \leq N-1 \\ 0, & \text{if } n \geq N, \end{cases}$$

$$n, k = 0, 1, \ldots, P-1.$$

Now the assumption of periodicity R(n) with period P is permissible. Then we have

$$\hat{f}_k = F^{-1}[\tilde{\bar{S}}_j(P) \cdot \tilde{R}_j(P)],$$

from which it follows that to calculate sum (1) it is necessary to carry out $P(3 \log_2 P + 2)$ operations.

The given formulas for calculating the number of operations still do not determine the economy of one method or another. The formal index A that characterizes the economy of a method is the number of operations per unit of area of the surface to be evaluated.

The indices obtained above for the number of operations must be normalized to a quantity proportional to L_0. According to the equal observation principle, the quantity L_0 is related to L_r, viz.:

$$L_0 \leq L_\phi - L_r. \qquad (2)$$

Using the notation $P/N = \tau$, we write

$$L_0 = \tau L_r,$$

whence

$$L_r \leq \frac{\sqrt{2n-1}}{1+\tau} \cdot L_{3\varphi}^{(1)}, \qquad (3)$$

where $L_{зф}^{(m)}$ is the width of the m-th Fresnel zone, equal to

$$L_{з.р}^{(m)} = \sqrt{2m-1}\, L_{з.р}^{(1)},$$

and u is the number of the Fresnel zone corresponding to the edge of the radiation pattern.

In accordance with the condition of impermissibility of frequency superposition [Ref. 3], the number of readings N on interval L_r must satisfy the inequality

$$N > \frac{L_r}{\delta_к}, \tag{4}$$

where $\delta_к$ is the discretization step equal to $\frac{1}{2}(\sqrt{2u-1} - \sqrt{2u-3})$.

Based on formulas (2), (3) and (4), we have

$$N \geqslant 2\frac{\sqrt{2u-1} - \varepsilon}{\sqrt{2u-1} - \sqrt{2u-3}} \tag{5}$$

$$\varepsilon = L_{\varepsilon} / L_{з.р}^{(1)}.$$

The resultant formula is a generalization to the case $\varepsilon \neq 0$ of the well known rule of complex signal theory: the product of the signal band (denominator in (5) -- B. M.) multiplied by its duration (numerator in (5) -- B. M.) is equal to the number of readings of the discretized signal [Ref. 2], which is valid only for $\varepsilon = 0$.

It can be proved that

$$\lim_{u \to \infty} \left(\sqrt{2u-1} - \frac{1}{\sqrt{2u-1} - \sqrt{2u-3}}\right) = 0$$

From this, using (3) and (5), we get the asymptotic equality

$$L_r = \frac{N^{1/2}}{\sqrt{2(1+\tilde{\varepsilon})}}\, L_{з.р}^{(1)} \tag{6}$$

or

$$L_r = \sqrt{\frac{\tilde{\varepsilon}}{2(1+\tilde{\varepsilon})}} \cdot N^{1/2} L_{з.р}^{(1)}.$$

Then

$$\frac{2}{L_{з.р}^{(1)}} \cdot \sqrt{2(1+\tilde{\varepsilon})}\, N^{1/2} L_{зф}^{(1)} \text{ for the direct method,}$$

$$\left.\begin{aligned} &\frac{1}{L_{2p}^{(1)}}\cdot\frac{\sqrt{2(1+\tau)}}{\tau}\cdot N^{1/2}(3\log_2 N+2), \text{ if } \tau<1\\ &\frac{1}{L_{2p}^{(1)}}\cdot\sqrt{2(1+\tau)}\cdot N^{1/2}(3\log_2 N+2), \text{ if } \tau>1 \end{aligned}\right\}$$ for the method of fast Fourier transforms

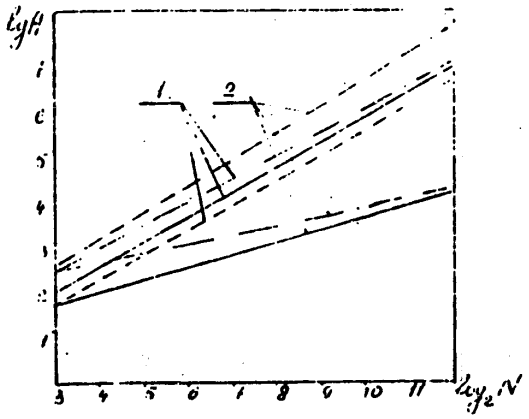

Fig. 1. Number of operations A per unit of surface as a function of the number of readings on the interval L_r of signal observation with use of the direct method (1) and the fast Fourier transform method (2) for values of $\tau = 1/N$ (- - - - -), 1 (———) and 7.0 (—• — •— •—)

The resultant relations imply (Fig. 1) that when using systems with one or a few readings ($L_0 \approx 0$) the direct method is preferable, the advantage of the method of fast Fourier transforms increasing with N. When a many-reading system is used, beginning at some value $\tau > 1/N$, the fast Fourier transform method has the advantage over the direct method at any values of N. Analysis of the relation $A = f(\tau)$ shows that when $\tau \approx 1$, the method of fast Fourier transforms gives the maximum gain compared with the direct method for any N (Fig. 2).

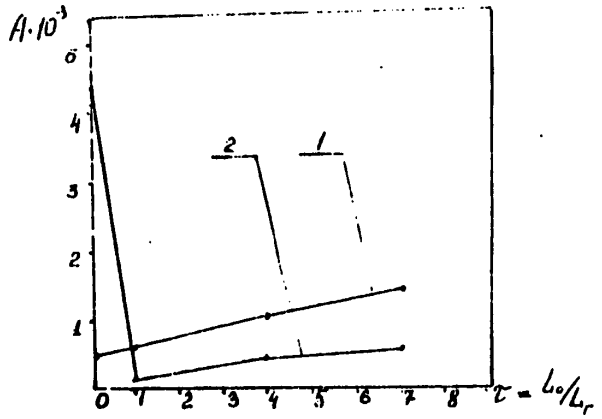

Fig. 2. Number of operations A per unit of area as a function of the ratio L_0/L_r for N = 32 when using the direct method (1) and the fast Fourier transform method (2)

In the case of limited processing intervals considerably smaller than L_G, 2^x-stage signal processing can be used [Ref. 4] in which so-called preweighted accumulation on the first stage limits the band of the signal S(t), and the main processing is done on the second stage. Such a structure reduces requirements for speed of processor devices. In this case the considerations given above concerning A are suitable for each of the processing stages individually. Let us analyze the necessary productivity A for 2^x-stage processing. On the first stage, the parameter $\tau = 1/N_{пр}$ ($N_{пр}$ is the number of readings of the input signal) is small, and consequently on the first stage the direct method has an obvious advantage over the method of fast Fourier transforms. On the second stage the parameter $\tau = P/\nu_L$ (ν_L is the number of signal readings at the input of the second stage). On the whole, the productivity A for the 2^x-stage processing can be written as

$$A = \nu_L A^{(1)} + A^{(2)}$$

where $A^{(1)}$ and $A^{(2)}$ are the numbers of operations on the first and second processing stages per unit of area of the reflective surface function to be evaluated. Based on the above discussion, we can write for the direct method:

$$\nu_L > 2(1+\tau)\left(\frac{L_r}{L^{(1)}_{эф}}\right)^2,$$

$$A^{(1)} = \frac{2N_{пр}}{L_0} > \frac{2N_{пр}\sqrt{2(1+\tau)}}{\tau \nu_L^{1/2} L^{(1)}_{эф}},$$

$$A^{(2)} = \frac{2\nu_L P}{L_0} = \frac{8(1+\tau)^2}{L^{(1)}_{эф}} \cdot \left(\frac{L_r}{L^{(1)}_{эф}}\right)^2,$$

and for the method of fast Fourier transforms

$$\frac{\nu_L(3\log_2\nu_L+2)}{L_0} = \frac{2(1+\tau)}{\tau}\cdot\frac{L_r}{(L^{(1)}_{эф})^2}\left[3\log_2(1+\tau)+6\log_2\frac{L_r}{L^{(1)}_{эф}}+5\right], \text{ if } \tau \leqslant 1,$$

$$\frac{\tau\nu_L(3\log_2\tau\nu_L+2)}{L_0} = 2(1+\tau)\frac{L_r}{(L^{(1)}_{эф})^2}\left[3\log_2(1+\tau)+6\log_2\frac{L_r}{L^{(1)}_{эф}}+5\right], \text{ if } \tau > 1.$$

Analysis of these functions shows the presence of an optimum for the function $A = f(\tau)$ at fixed values of L_r and $L^{(1)}_{эф}$. Calculations show that for different values of these parameters the quantity τ may differ considerably from 1, and the gain from using the fast Fourier transform method becomes less pronounced than for one-stage processing. Thus the selection of the method of calculating correlation sums must be accompanied by computation of κ in each specific case.

I thank L. S. Al'tman for constructive discussion of the matters considered in this paper.

REFERENCES

1. Leith, "Quasi-Holographic Methods in Microwave Band" in: "Primeneniye golografii [Using Holography], edited by J. Goodman, Moscow, "Mir", 1973.

2. Rabiner, L., Gold, B., "Teoriya i printsipy tsifrovoy obrabotki signalov" [Theory and Principles of Digital Signal Processing], Moscow, "Mir", 1978.

3. Hamming, R. W., "Chislennyye metody" [Numerical Methods], Moscow, "Nauka", 1968.

4. Brown, W. M., Houser, G. G., Jenkins, R. E., "Synthetic Aperture Processing with Limited Storage and Presumming", IEEE TRANSACTIONS ON AEROSPACE AND ELECTRONIC SYSTEMS, Vol AES-9, No 2, March, 1973.

UDC 21.391.266

SYNTHESIZING QUASI-HOLOGRAPHIC SYSTEM ADAPTIVE TO REFLECTING SURFACE

[Article by B. S. Mush]

[Text] The paper notes difficulties in practical realization of optimum methods of solving the principal equation of a quasi-holographic system that are related to absence of a priori data and in large measure are eliminated when algorithms are used that are adaptive to a reflective surface function. The principal equation of a pulse-Doppler quasi-holographic system is given with its optimum solution in the sense of the minimum rms deviation of the estimate of the reflective surface function from its exact value. An algorithm is described that is adaptive to the operator's signal when the structure of the operator is identical to that of an optimum operator and realizes an iterative procedure of successive approximations. The article presents the proof of convergence of the iterative procedure and gives the results of a numerical experiment on studying effectiveness of the constructed adaptive algorithm.

Optimum methods of solving the principal equation of a quasi-holographic system [Ref. 1, 2], despite all their advantageous properties in the sense of estimation of the reflective surface function f, cannot be realized in covering real surfaces, since in most cases even the energy spectra of the reflective surface function are a priori unknown. However, optimum operators enable us on the one hand to synthesize suboptimum and adaptive algorithms that improve the estimate of the reflective surface function by "signal tuning", and on the other hand to evaluate the quality of these algorithms with respect to the degree that the estimate approximates the optimum. The problem of constructing an adaptive algorithm should be considered solved if "we manage to construct algorithms... that use only realizations accessible to measurement" [Ref. 3].

Taking our lead from Ref. 2, we write the principal equation as

$$\int_{-\infty}^{\infty} K[X(t)-x]\, f(x,\bar{y})\,dx = s(t)\cdot \exp 2ik\,y(t) + n(t), \qquad (1)$$

where S(t) is the signal at the input of the antenna system,

$$K(x) = G^2\left(\frac{x}{y(t)}\right)\cdot \exp -ik\frac{x^2}{y(t)},$$

X(t) and Y(t) are projections of the trajectory of the phase center of the radiating and reception systems with polar pattern G(x/y(t)) on the x and y axes of the coordinate system fixed to the reflecting surface, $k = 2\pi/\lambda$, λ is the wavelength of the system, n(t) are noises of the system, $\bar{y} = \frac{c}{2}\theta + y(t)$, $\theta = t - T_n$, T_n is the repetition period, and n is the probe number.

In the following we will examine equation (1) as an integral equation of the first kind, and treat its solution as a formalized target of a quasi-holographic system.

The optimum estimate $\hat{f}$ of the reflective surface function can be found by using the Wiener-Kolmogorov operator with kernel R_{opt} [Ref. 2, 4]:

$$\hat{f}(x,\bar{y}) = \int_{(T)} R_{opt}[x-X]\cdot s(t)\cdot \exp 2ik\,y(t)\,dt,$$

where

$$R_{opt}(x) = \int_{-\infty}^{\infty} \frac{\tilde{K}^*(\rho)}{\beta(\rho) + |\tilde{K}(\rho)|^2} \exp i\rho x\, d\rho,$$

$\beta(p) = N(p)/|\tilde{f}(p)|^2$, N(p) is the energy spectrum of n(t), T is the processing period, the symbols (~) and (*) denote the Fourier transform and the complex conjugate respectively, or in the form of the spectrum of the estimate

$$\tilde{\hat{f}}(\rho) = \frac{\nu_{opt}(\rho)}{\tilde{K}(\rho)}\cdot \tilde{s}(\rho), \qquad (2)$$

where ν_{opt} is the optimum value of the Tikhonov stabilizing factor [Ref. 4] which is equal to

$$\nu_{opt}(\rho) = \frac{|\tilde{f}(\rho)|^2\cdot|\tilde{K}(\rho)|^2}{N(\rho) + |\tilde{f}(\rho)|^2\cdot|\tilde{K}(\rho)|^2} \leq 1. \qquad (3)$$

A special case of the optimum operator when $\beta(p) >> \mathrm{Max}|\tilde{K}(p)|$ is an operator of the type "matched to a point object":

$$\tilde{R}(x) \sim \int_{-\infty}^{\infty} \tilde{K}^*(\rho)\cdot \exp i\rho x\, d\rho. \qquad (4)$$

Let us now consider the structure of an adaptive operator. Let us have a zero approximation of the estimate of the reflective surface function $\tilde{\hat{f}}_0(x)$ that can be obtained by an operator that does not depend on the reflective surface function or noise, e. g. of type (4). Let us call the function $\tilde{\hat{f}}_n(x)$ the estimate of the reflective surface function in the n-th approximation. The Fourier transform of this function takes the form

$$\tilde{\hat{f}}_n(\rho) = \frac{\nu_{opt}^{(n)} \cdot \tilde{s}(\rho)}{\tilde{K}(\rho)} = \frac{|\hat{f}_{n-1}|^2 \cdot \tilde{K}^*(\rho)}{N(\rho) + |\hat{f}_{n-1}|^2 \cdot |\tilde{K}(\rho)|^2} \cdot \tilde{s}(\rho), \qquad (5)$$

where $\nu_{opt}^{(n)}$ is obtained from formula (3) by replacing $|\tilde{f}|$ by its (n - 1)-th approximation, and n = 0, 1, 2,... This formula, combined with the formula that assigns $\tilde{\hat{f}}_0$, describes the iteration procedure. Let us prove existence of convergence of the sequence to a limit that in the sense of rms deviation is closer to $\tilde{f}$ than any estimate $\tilde{\hat{f}}_n$ at least at a sufficiently low noise level.*

We assume that

$$\tilde{\hat{f}}_c = \tilde{K}^* \cdot \tilde{s},$$

then

$$\tilde{\hat{f}}_1 = \frac{|\tilde{K}|^2 \tilde{K}^* \cdot |\tilde{s}|^2}{N + |\tilde{K}|^4 \cdot |\tilde{s}|^2} \cdot \tilde{s}.$$

Let us consider the positive definite function

$$\Theta_{0,1}(\rho) = \frac{|\tilde{f} - \tilde{\hat{f}}_0|}{|\tilde{f} - \tilde{\hat{f}}_1|}.$$

If $\Theta_{0,1}(p) > 1$, the first-approximation estimate of the reflective surface function on the interval of assignment of spatial frequencies p gives a gain in the sense of rms deviation as compared with the zero-approximation estimate.

We can see from the expressions for $\tilde{\hat{f}}_0$ and $\tilde{\hat{f}}_1$ that

$$\Theta_{0,1}(\rho) = \left| \frac{1 - |\tilde{K}|^2}{1 - \frac{|\tilde{K}|^4 \cdot |\tilde{s}|^2}{N + |\tilde{K}|^4 \cdot |\tilde{s}|^2}} \right|,$$

which implies that the function $\Theta_{0,1}(p) \to \infty$ as $N \to 0$.

Analogous arguments are valid for an arbitrary function $\Theta_{n-1,\,n}$. Consequently, at least for a sufficiently low noise level, the n-th estimate of the reflective surface function gives a gain compared with the (n - 1)-th estimate.

*An operator of type (4) is optimum at high noise level.

To verify the conclusions drawn above, a computational experiment was done. The conditions of the experiment consisted in assigning the reflective surface function as a data file of complex numbers $f(\ell)$, $\ell = 0, 1, \ldots, N-1$ with Rayleigh distribution of the modulus and uniform distribution of the phase on interval $[-F, F]$. The signal was formed in accordance with equation (1). The estimate $\hat{f}_n(\ell)$ of the reflective surface function was calculated from formulas (2) and (5). Quantitatively, the quality of the estimate was defined by the quantity B calculated from the formula

$$B(n) = \left(\frac{1}{2}\sum_{\ell=0}^{N-1}\left|\frac{|f(\ell)|}{\|f\|} - \frac{|\hat{f}_n(\ell)|}{\|\hat{f}_n\|}\right|\right)^{1/2},$$

where $0 \leqslant B \leqslant 1$.

The function n(t) in (1) was simulated by an uncorrelated number sequence, and the noise level was assigned by the quantity γ:

$$\gamma = \frac{|\tilde{f}|^2 \cdot |\tilde{K}(p)|^2}{\tilde{N}(p)},$$

where the symbol $\tilde{(\ )}$ denotes averaging of the sample.

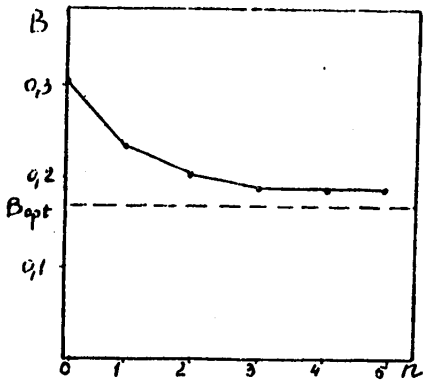

Normalized rms deviation of the estimate of the reflective surface function as dependent on the number n of the step in the iterative procedure of the adaptive algorithm

The figure shows the results of the experiment for $\gamma = 100$. The experiment demonstrated convergence of the procedure described above, in which there is an appreciable gain in quality of the estimate of the reflective surface function up to the fourth step of the iteration.

I thank Yu. V. Kuznetsova and I. V. Garina for their contribution in doing the experiment.

REFERENCES

1. Kondratenkov, G. S., "Synthesizing an Optimum Method of Processing Radio Holograms", RADIOTEKHNIKA, Vol 33, No 5, 1978.

2. Mush, B. S., "Synthesizing Artificial Aperture for Microwave Radio Holograms Reflected from the Surface of the Sea", RADIOTEKHNIKA I ELEKTRONIKA, Vol 25, No 7, 1980.

3. Tsipkin, Ya. Z., "Osnovy teorii obuchayushchikhsya sistem" [Principles of the Theory of Learning Systems], Moscow, "Nauka", 1970.

4. Tikhonov, A. N., Arsenin, V. A., "Metody resheniya nekorrektnykh zadach" [Methods of Solving Incorrect Problems], Moscow, "Nauka", 1974.

UDC 621.396.67.001.24:778.38

DETERMINING INTERCOUPLING OF SPATIALLY COMBINED ANTENNAS BY RADIO HOLOGRAPHY METHODS

[Article by R. A. Orlov]

[Text] A method is considered for determining the mutual immittance between two spatially combined reciprocal antennas. The method is based on using radio holograms recorded on a closed reference surface covering the interacting atnennas. A basis is proposed for describing the radio holograms with arbitrary distance of a spherical reference surface from the antenna to be analyzed. A solution is given for the problem of finding the immittance of two collinear dipole antennas.

Finding the mutual coupling between antennas that are spatially combined in the limits of a single radio engineering complex, or between elements of the same antenna system is a problem of considerable current interest both for analyzing electromagnetic compatibility and in the design of complex antenna facilities. An examination of the voluminous research devoted to solution of this problem shows that the measure of intercoupling in all these cases is the mutual impedance determined by various methods, including the method of induced emf's [Ref. 1], the method of the angular spectrum of plane waves [Ref. 2], etc. However, all these methods make essential use of the structure of the interacting antennas, which at times is a severe impediment to solution of the formulated problem, especially when it involves antennas of different types. A way out of this situation might be to use a method of analyzing intercoupling relying only on the distribution of the electromagnetic field set up by the antennas being studied on some surface in the vicinity of the facility on which they are installed, i. e. a method that utilizes radio holograms of the fields of radiation of the antennas. The reference surface must be situated in the near zone of the antenna system to be analyzed, and the algorithm for calculating mutual impedance must enable simple and effective use of computers.

These requirements are most simply realized if the analysis of intercoupling uses a law of conservation of electromagnetic energy in the space that contains the interacting antennas [Ref. 3]. This law can be written as

$$\sum_{i,k=1}^{N}\left\{\oint_S([\mathbf{E}_k,\mathbf{H}_i^*],\mathbf{n})\,dS+\int_V\left(\mathbf{E}_k\frac{\partial\mathbf{E}_i^*}{\partial t}+\mathbf{H}_k\frac{\partial\mathbf{H}_i^*}{\partial t}\right)dV\right\}+\sum_{k=1}^{N}\int_V(\mathbf{I}_k,\mathbf{E}_k^*)\,dV=0, \quad (1)$$

where $\vec{E}_{i,k}$, $\vec{H}_{i,k}$ are fields set up by antennas "i" and "k" at an arbitrary point of the volume V bounded by surface S; $\vec{n}$ is the unit outer normal to surface S; I_k are the currents in the antennas; N is the number of interacting antennas. The surface integral in the braces in (1) defines the flow of energy from all sources to the surrounding space, and the volume integral defines the total energy of the overall electromagnetic field stored in V. The last term characterizes the balance of the powers in each of the interacting antennas as determined by the power fed to the antenna from the oscillator, and the sum of the partial powers induced in this antenna by all other radiators.

Let us assume for the sake of simplicity that the interacting antennas are located in free space, and that the radiated fields are monochromatic and are linear functions of their generated current distributions. Then, representing the values of the powers in each radiator as the product of currents I_k multiplied by the equivalent applied voltages U_k (comprised of the excitation voltages and the sum of the induced emf's), writing the system of equations for the currents in the antennas with consideration of their mutual impedances, where the corresponding U_k are in the second members of these equations, and solving this system with respect to impedances, we get the following expression for the mutual impedance of an arbitrary pair of radiators:

$$\begin{aligned}
&\mathcal{Z}_{ik}=\mathcal{Z}_{ik}^{(1)}+\mathcal{Z}_{ik}^{(2)};\\
&\mathcal{Z}_{ik}^{(1)}=\frac{1}{2}\oint_S\left(\left\{[\mathbf{E}_k',\mathbf{H}_i^{*'}]+[\mathbf{E}_k^{*'},\mathbf{H}_i']\right\},\mathbf{n}\right)dS;\\
&\mathcal{Z}_{ik}^{(2)}=\frac{i\omega}{2}\int_V\left\{(\mathbf{E}_i',\mathbf{E}_k^{*'})+(\mathbf{E}_i^{*'},\mathbf{E}_k')+(\mathbf{H}_i',\mathbf{H}_k^{*'})+(\mathbf{H}_i^{*'},\mathbf{H}_k')\right\}dV,
\end{aligned} \quad (2)$$

where the primes denote fields set up by antennas in which the current distribution is normalized to unity.

An examination of expressions (2) shows that radio holographic information can be used only to find the component $z_{ik}^{(1)}$ determined by distributions of the fields of radiation of the antennas over the surface S that encompasses these antennas. Moreover, we can readily see that to get this component it is sufficient to integrate the radio hologram obtained by using the field distribution of the other interacting antenna as a reference signal. However, there are considerable difficulties involved in directly producing such radio holograms, and it is preferable in this problem to use holographic information in the form of distributions of the amplitude and phase of the field of radiation of each of the antennas individually. Such information also enables us

to find the parameters of the antennas with consideration of their interaction and conforms to present-day methods of recording holograms in the radio wave band.

Sequential registration of radio holograms assumes storage of data files on amplitude, phase and polarization of the field over the entire surface S, i. e. a large volume of operating computer memory, a requirement that increases with increasing ratio between the linear dimensions of the investigated antenna system and the wavelength of the radiated field, and involves a cumbersome procedure of successive computations with the use of these data files. Therefore when finding $z_{ik}^{(1)}$ it is desirable to use a method of field representation that sharply reduces the volume of stored information while retaining data about the radio hologram on the entire surface S and to describe the field distribution at an arbitrary distance from the antennas (including in the near zone), which corresponds to conditions of radio hologram registration on measurement stands.

The simplest closed surface is that of a sphere; when such a surface is used as S, we can represent the ampliphase distribution of the field on S as an expansion with respect to spherical vector wave functions [Ref. 4]:

$$\begin{aligned} \mathbf{H}'_k &= \sum_{\ell=0}^{\infty}\sum_{m=-\ell}^{\ell}\left\{ f'_{\ell m}(r)\mathbf{X}_{\ell m}(\theta,\varphi) - \frac{i}{k}\,\mathrm{rot}\left[g'_{\ell m}(r)\mathbf{X}_{\ell m}(\theta,\varphi)\right]\right\};\\ \mathbf{E}'_k &= \sum_{\ell=0}^{\infty}\sum_{m=-\ell}^{\ell}\left\{ \frac{i}{k}\,\mathrm{rot}\left[f'_{\ell m}(r)\mathbf{X}_{\ell m}(\theta,\varphi)\right] + g'_{\ell m}(r)\mathbf{X}_{\ell m}(\theta,\varphi)\right\}; \end{aligned} \tag{3}$$

where

$$\mathbf{X}_{\ell m}(\theta,\varphi) = \frac{1}{\sqrt{\ell(\ell+1)}}\,\mathbf{L}\,Y_{\ell m}(\theta,\varphi)\ ;\quad \mathbf{L} = -i\,[\mathbf{r},\nabla]$$

is a vector differential operator; $Y_{\ell m}(\theta,\phi)$ are scalar spherical harmonics that take the form

$$Y_{\ell m}(\theta,\varphi) = \left[\frac{2\ell+1}{4\pi}\,\frac{(\ell-m)!}{(\ell+m)!}\right]^{1/2} P_\ell^m(\cos\theta)\exp\{im\varphi\}.$$

Outside of the sources, the radial functions can be written in the form

$$f'_{\ell m}(r) \equiv a'_E(\ell,m)\,h_\ell^{(1)}(kr)\ ;\quad g'_{\ell m}(r) \equiv a'_M(\ell,m)\,h_\ell^{(1)}(kr), \tag{4}$$

where $h_\ell^{(1)}(kr)$ are spherical Hankel functions, and the coefficients $a'_E(\ell,m)$ and $a'_M(\ell,m)$ in the general case are defined by the following formulas:

$$\begin{aligned} a'_E(\ell,m) &= \frac{4\pi k^2}{i\sqrt{\ell(\ell+1)}}\int_V Y^*_{\ell m}(\theta,\varphi)\left\{\rho'\frac{d}{dr}\left[r\,j_\ell(kr)\right] + \right.\\ &\left. + \frac{ik}{c}\,(\mathbf{r},\mathbf{I}')\,j_\ell(kr) - ik\,\mathrm{div}\left([\mathbf{r},\mathbf{M}]\right)j_\ell(kr)\right\}dV;\\ a'_M(\ell,m) &= \frac{4\pi k^2}{i\sqrt{\ell(\ell+1)}}\int_V Y^*_{\ell m}(\theta,\varphi)\left\{\mathrm{div}\left(\frac{1}{c}\,[\mathbf{r},\mathbf{I}']\right)j_\ell(kr) + \right.\\ &\left. + \mathrm{div}\,\mathbf{M}\,\frac{d}{dr}\left[r\,j_\ell(kr)\right] - k^2(\mathbf{r},\mathbf{M})\,j_\ell(kr)\right\}dV, \end{aligned} \tag{5}$$

in which $j_\ell(kr)$ are spherical Bessel functions of the first kind, integration is carried out only over the region that contains the sources, and $\vec{M}$ denotes magnetic current density. In practice, these expressions are considerably simplified since $\vec{M} \equiv 0$, and the charges and currents are related by the equation of continuity.

The given expansions are valid at an arbitrary distance from sources of radiation with the exception of a sphere of minimum radius that contains the system of interacting antennas and is determined by the maximum overall dimensions of this system. Thus, assuming that the surface S has the form of a sphere of radius R, substituting (3) in (2) and considering the absolute convergence of the series with respect to vector spherical harmonics, as well as the conditions of orthogonality for these series and the fact that the normal $\vec{n}$ coincides with the radial unit vector $\vec{r}_0$ of the spherical coordinate system, we find

$$z_{ik}^{(1)} = \frac{iR^2}{2k} \sum_{\ell=0}^{\infty} \sum_{m=-\ell}^{\ell} \left\{ \frac{1}{R} \left[g_{k\ell m}^{\prime *} g_{i\ell m}^{\prime} - g_{k\ell m}^{\prime} g_{i\ell m}^{\prime *} + f_{k\ell m}^{\prime} f_{i\ell m}^{\prime *} - f_{i\ell m}^{\prime} f_{k\ell m}^{\prime *} \right] + g_{k\ell m}^{\prime} \frac{dg_{i\ell m}^{\prime *}}{dr}\Big|_{r=R} - g_{k\ell m}^{\prime *} \frac{dg_{i\ell m}^{\prime}}{dr}\Big|_{r=R} + f_{i\ell m}^{\prime} \frac{df_{k\ell m}^{\prime *}}{dr}\Big|_{r=R} - f_{i\ell m}^{\prime *} \frac{df_{k\ell m}^{\prime}}{dr}\Big|_{r=R} \right\}. \quad (6)$$

Now let us consider the contribution made by the real and imaginary components to the quantity $z_{ik}^{(1)}$. To do this, we will assume that the surface S is situated rather far away (radius R is large) and we will use an asymptotic representation for the spherical Hankel function at large values of the argument. Then we get the expression

$$z_{ik}^{(1)} \approx \frac{1}{2k^2} \sum_{\ell=0}^{\infty} \sum_{m=-\ell}^{\ell} \left\{ \left[a_{kH}^{\prime} a_{iH}^{\prime *} + a_{kH}^{\prime *} a_{iH}^{\prime} + a_{i\theta}^{\prime} a_{k\theta}^{\prime *} + a_{i\theta}^{\prime *} a_{k\theta}^{\prime} \right] + \frac{2i}{kR} \left[a_{kH}^{\prime *} a_{iH}^{\prime} - a_{iH}^{\prime} a_{iH}^{\prime *} + a_{k\theta}^{\prime} a_{i\theta}^{\prime *} - a_{i\theta}^{\prime} a_{k\theta}^{\prime *} \right] \right\}. \quad (7)$$

from which we can see that the component of mutual impedance $z_{ik}^{(1)}$ in the general case has a reactive component that approaches zero as radius R increases. Carrying out an analogous study of the other part of the mutual impedance that differs only in the fact that integration in this case is carried out over the space external to a sphere of large radius, we can establish the purely reactive nature of component $z_{ik}^{(2)}$.

Thus, radio holographic information enables direct determination only of the resistive component of mutual impedance between spatially combined antennas. Let us deal briefly with finding the reactive component of mutual impedance $\operatorname{Im} z_{ik}$. Here as a rule we use indirect methods based on utilizing additional information concerning the resistive component of mutual immittance, and namely the way that $\operatorname{Re} z_{ik}$ depends on electrical distance between antennas or on frequency.

The first such method makes use of the fact that the dependence of $\mathrm{Re}\, z_{ik}$ on spatial separation of the antennas is oscillatory and vanishes at values of the phase of z_{ik} equal to $\psi = -\pi/2 - \pi(k-1)$ [Ref. 5]. Taking these points as nodes of interpolation, we can find the phase function of mutual impedance, the modulus of z_{ik} and then $\mathrm{Im}\, z_{ik}$. At small distances between antennas, the phase function is determined by extrapolation only to the middle of the "main lobe" of the function $\mathrm{Re}\, z_{ik}$, since in a close approach the inductive and static fields of the antennas begin to make the major contribution to the reactive component of z_{ik}.

The second method uses the frequency dependence of the resistive component of mutual impedance $\mathrm{Re}\, z_{ik}(\omega)$. While a similar approach was suggested in Ref. 3, the method considered there for determining the frequency dependence of the Green's function and subsequent summation with consideration of the distributions of currents and charges as well as the configuration of the antennas to get the complete reactive component of z_{ik} is rather awkward and complicated. Besides, it is completely unsuitable if we are using only radio holographic information. Therefore when finding $\mathrm{Im}\, z_{ik}$ it is advisable to use direct reconstruction of this component from the dependence $\mathrm{Re}\, z_{ik}(\omega)$ based on algorithms available in the literature [Ref. 6]. The resultant error due to the fact that in the general case the system of interacting antennas is not a minimal-phase system in view of the presence of multiple scattering is a small error, and the accuracy obtained in any event is no poorer than in the method of induced emf's that accounts for only one-time interactions.

In conclusion, we give a solution for the problem of determining mutual impedances of two thin dipoles of arbitrary length. Let the antennas be situated on segments $z \in [a, b]$, $z \in [-a, -b]$ of the z-axis, and let them have small gaps in the center for excitation. We take the current distribution to be the same in the antenna systems, and we assume that this distribution is described by an even function of z and vanishes on the ends of the antenna. Since the currents are radial, $[\vec{r}, \vec{I}] = 0$, and all components of magnetic multipoles are equal to zero. The current density appearing in expression (5) is determined in spherical coordinates for $r \in [a, b]$, and in the case of harmonic time dependence, it can be written as

$$I_{1,2}(r) = \frac{I_0}{2\pi r^2} I'_{1,2}(r)\, \delta(\cos\theta \mp 1)\, \exp\{-i\omega t\}, \qquad (8)$$

where δ is the Dirac delta function. Determining the charge distirbution on the basis of the equation of continuity, and calculating the integrals appearing in (5) over θ and ϕ, we find as already noted in Ref. 4 that for such antennas only multipoles with indices $m = 0$ are excited. To calculate the radial integral we must know the current distribution along the antenna normalized to the maximum. Considering that this distribution can be represented as a Fourier expansion, and for the sake of simplicity taking $I_{1,2}(r)$ as coincident with only one spatial harmonic of the expansion, the remaining integral can be computed fairly easily, yielding

$$a'_e(l,0) = \frac{2k}{c}\left[\frac{4\pi(2l+1)}{l(l+1)}\right]^{1/2}\left\{k(a+b)j_e\left(\frac{k}{2}(a+b)\right) - ka\,j_e(ka) - kb\,j_e(kb)\right\}. \qquad (9)$$

The general expression for the active component of mutual impedance in the given case takes the form:

$$R_{12} = \frac{1}{2k^2}\sum_{e=1}^{\infty}\left\{a_{1e}\overline{a_{2e}^{1*}} + \overline{a_{1e}^{1*}}\,a_{2e}^{1}\right\}.$$

Substituting expression (9) in this expression, we get the following relation for calculating the resistive component of immittance of the two antennas:

$$\overline{R_{12}} = \frac{2\pi}{c^2}\sum_{e=1}^{\infty}\frac{2e+1}{e(e+1)}\left\{k^2(a+b)^2 j_e'^2\left(\frac{k}{2}(a+b)\right) + k^2a^2 j_e'^2(ka) + k^2b^2 j_e'^2(kb) - 2k^2a(a+b)j_e(ka)j_e\left(\frac{k}{2}(a+b)\right) - 2k^2b(a+b) j_e(kb)j_e\left(\frac{k}{2}(a+b)\right) + 2k^2ab\,j_e(ka)j_e(kb)\right\}. \quad (10)$$

In accordance with expression (10), calculations of R_{12} were done for dipoles of length $\lambda/4$ as a function of the electrical distance $2a/\lambda$ between antennas. Comparison of the results of the calculation with a curve for the mutual resistance under the same conditions calculated by the method of induced emf's [Ref. 1] showed that both solutions give similar relations for R_{12}. Maximum discrepancy is no more than 5% with 10 terms retained in the series. It should be noted that when the distance between dipoles is increased a greater number of terms must be considered, involving an increase in the radius R_0 of the sphere that contains these antennas, which agrees completely with results obtained previously on the necessity of accounting for terms with indices $\ell \geq kR_0$ in calculations [Ref. 7].

REFERENCES

1. Lavrov, G. A., "Vzaimnoye vliyaniye lineynykh vibratornykh antenn" [Mutual Influence of Linear Dipole Antennas], Moscow, "Svyaz'", 1975.

2. Deshpande, M. D., Das, B. N., "A New Approach to the Mutual Immitance Between Two Radiators", J. INT. ELECTRON. AND TELECOMMUN. ENG., Vol 23, No 6, 1977, pp 359-364.

3. Vendik, O. G., "Determining Mutual Impedance Between Antennas From Known Radiation Patterns in the Far Zone", RADIOTEKHNIKA, Vol 17, No 10, 1962, pp 11-20.

4. Jackson, J., "Klassicheskaya elektrodinamika" [Classical Electrodynamics], Moscow, "Mir", 1965.

5. Sazonov, D. M., "Raschet vzaimnykh impedansov proizvol'nykh antenn po ikh diagrammam napravlennosti" [Calculating Mutual Impedances of Arbitrary Antennas From Their Radiation Patterns], RADIOTEKHNIKA I ELEKTRONIKA, Vol 15, No 2, 1970, pp 376-378.

6. Gadel'shin, R. M., Golubkov, A. G., Gonostarev, V. A., "Method of Determining the Phase-Frequency Response of a Minimum-Phase Target From the

Amplitude-Frequency Response Assigned in a Limited Frequency Band", IZVESTIYA VYSSHIKH UCHEBNYKH ZAVEDENIY: RADIOELEKTRONIKA, Vol 22, No 3, 1979, pp 89-92.

7. Ludwig, A. C., "Near-Field Far-Field Transformations Using Spherical Wave Expansions", IEEE TRANSACTIONS ON ANTENNAS AND PROPAGATION, AP-19, No 2, 1971, pp 214-220.

UDC 535.317.1

MEASURING PARAMETERS OF SCATTERING BODIES BY RADIO HOLOGRAPHY METHOD

[Article by A. Ya. Pasmurov]

[Text] An edge wave method [Ref. 1] is used to get analytical relations for calculating the scattering characteristics of individual "shining" points of an ideally conductive cylinder of finite dimensions. On this basis an equation is derived for a a standard complex Fourier radio hologram, and a test algorithm is developed for modeling the radio holographic process. It is shown that the potential accuracy of measuring the effective scattering surface of "shining" points of an object by the method of Fourier radio holography can be brought to 0.5 dB.

The results of theory, modeling and experiment are compared, and recommendations are made on standardizing measurements of local scattering characteristics of bodies.

To solve various applied problems in diffraction of electromagnetic waves in the high-frequency approximation requires diagrams of the effective scattering surface of individual "shining" points of an object. Such scattering characteristics, termed "local" [Ref. 2], can be obtained analytically or experimentally. It is advisable to use theoretical methods for calculating local scattering characteristics of ideally conductive bodies of simple geometric shape (cylinder, cone and the like). The local scattering characteristics of a complicated shape can be determined only experimentally as a rule. Methods of radio holography are used to do this, in particular the method of inverted synthesis of one-dimensional Fourier radio holograms by rotating the object around its center of mass [Ref. 3, 4].

A fundamental condition of doing experiments of this kind is the availability of a reference scatterer for which analytical expressions can be found that describe its local scattering characteristics. The reference is necessary for getting a quantitative measurement standard, for checking operation of the experimental facility by comparing theoretical and experimental data, and for evaluating the experimental error. In addition, the reference can be used to model the radio holographic process. The latter circumstance is the most important since the method of Fourier radio holography has a fundamentally inherent error of measurement of local scattering characteristics whose causes will be elucidated below. Comparison of results of theory and

modeling based on general analytical relations enables evaluation of the magnitude of this error, i. e. determination of the potential accuracy of the method. Comparison of the given results with experimental data enables determination of the instrumental error of a specific measurement facility.

Up until now, analysis of the method of radio holography has relied on use of a hypothetical body made up of a set of point scatterers [Ref. 3]. Obviously such an object cannot serve as a standard. In our paper, an ideally conductive cylinder of finite dimensions is taken as the reference scatterer. The edge wave method is used to get analytical expressions for calculating the local scattering characteristics of this reference. On the basis of these expressions, an equation is derived for a complex one-dimensional Fourier radio hologram, and a test algorithm is developed for modeling the radio holographic process.

Upon diffraction of a plane wave by an ideally conductive cylinder of length l and radius a (Fig. 1), a scattered field is formed in the far zone whose components for E- and H-polarization are respectively equal to [Ref. 1]:

$$E_\varphi = \frac{ia}{2} E_{0x} \frac{e^{ikR}}{R} \bar{\Sigma}(\vartheta, \vartheta_0), \quad (1)$$

$$E_\vartheta = \frac{ia}{2} H_{0x} \frac{e^{ikR}}{R} \Sigma(\vartheta, \vartheta_0), \quad (2)$$

where k is the wave number ($k = |\vec{k}_1| = |\vec{k}_s|$).

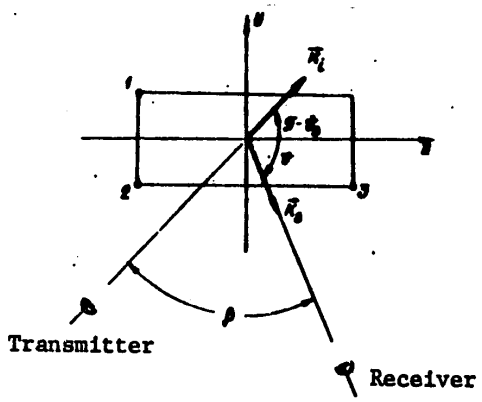

Fig. 1

In contrast to Ref. 1, the angle functions $\bar{\Sigma}(\theta,\theta_0)$ and $\Sigma(\theta,\theta_0)$ are represented in the form of three terms, each characterized by a corresponding scattering center of the cylinder (Fig. 1),

$$\bar{\Sigma}(\vartheta,\vartheta_0) = \bar{\Sigma}_1(\vartheta,\vartheta_0) + \bar{\Sigma}_2(\vartheta,\vartheta_0) + \bar{\Sigma}_3(\vartheta,\vartheta_0), \quad (3)$$

$$\Sigma(\vartheta,\vartheta_0) = \Sigma_1(\vartheta,\vartheta_0) + \Sigma_2(\vartheta,\vartheta_0) + \Sigma_3(\vartheta,\vartheta_0), \quad (4)$$

$$\overline{\Sigma}_1(\vartheta,\vartheta_0)=f_1[J_1(\xi_\vartheta)+iJ_2(\xi_\vartheta)]\,e^{i\frac{\kappa\ell}{2}(\cos\vartheta+\cos\vartheta_0)}, \tag{5}$$

$$\overline{\Sigma}_2(\vartheta,\vartheta_0)=f_2[-J_1(\xi_\vartheta)+iJ_2(\xi_\vartheta)]\,e^{i\frac{\kappa\ell}{2}(\cos\vartheta+\cos\vartheta_0)}, \tag{6}$$

$$\overline{\Sigma}_3(\vartheta,\vartheta_0)=f_3[-J_1(\xi_\vartheta)+iJ_2(\xi_\vartheta)]\,e^{-i\frac{\kappa\ell}{2}(\cos\vartheta+\cos\vartheta_0)}, \tag{7}$$

where J_1 and J_2 are Bessel functions of the first kind of first and second order respectively.

$$\xi_\vartheta=\kappa a(\sin\vartheta+\sin\vartheta_0).$$

For the functions $\Sigma_n(\theta,\theta_0)$ (n = 1, 2, 3) we can get expressions analogous to (5)-(7) by replacing the functions f_n with g_n defined by relations

$$\left.\begin{matrix}f_1\\g_1\end{matrix}\right\}=\frac{\sin\frac{\pi}{m}}{m}\left[\left(\cos\frac{\pi}{m}-\cos\frac{\vartheta-\vartheta_0}{m}\right)^{-1}\mp\left(\cos\frac{\pi}{m}-\cos\frac{\pi-\vartheta-\vartheta_0}{m}\right)^{-1}\right], \tag{8}$$

$$\left.\begin{matrix}f_2\\g_2\end{matrix}\right\}=\frac{\sin\frac{\pi}{m}}{m}\left[\left(\cos\frac{\pi}{m}-\cos\frac{\vartheta-\vartheta_0}{m}\right)^{-1}\mp\left(\cos\frac{\pi}{m}-\cos\frac{\vartheta+\vartheta_0}{m}\right)^{-1}\right], \tag{9}$$

$$\left.\begin{matrix}f_3\\g_3\end{matrix}\right\}=\frac{\sin\frac{\pi}{m}}{m}\left[\left(\cos\frac{\pi}{m}-\cos\frac{\vartheta-\vartheta_0}{m}\right)^{-1}\mp\left(\cos\frac{\pi}{m}-\cos\frac{2\pi-\vartheta-\vartheta_0}{m}\right)^{-1}\right], \tag{10}$$

$$m=3/2.$$

Expressions (3) and (4) are valid under condition that $\beta<\pi/2$ and $\pi/2+\beta<\theta_0<\pi$. Otherwise the number of terms in these equations may be less than three due to eclipsing of other scattering centers. Setting $\theta=\theta_0$ everywhere we can easily pass to the single-position case of observation ($\beta=0$). The resultant formulas enable calculation of the local scattering characteristics of an ideally conductive cylinder as a reference standard.

Simultaneously from equation (1) we can find the amplitude A_E and phase ϕ_E of the wave scattered by the object for E-polarization (analogous expressions follow from (2) for A_H and ϕ_H in the case of H-polarization):

$$A_E(\vartheta,\vartheta_0)=\frac{E_m}{2}\frac{a}{R}\operatorname{Mod}\overline{\Sigma}(\vartheta,\vartheta_0), \tag{11}$$

$$\varphi_E(\vartheta,\vartheta_0)=\kappa R+\pi/2+\operatorname{Arg}\overline{\Sigma}(\vartheta,\vartheta_0), \tag{12}$$

where Mod and Arg denote respectively the modulus and argument of the complex quantity $\overline{\Sigma}(\theta,\theta_0)$.

Using the latter equations and choosing the appropriate parameters of the reference wave, we get the following function of the complex reference Fourier radio hologram for an ideally conductive cylinder in the case of finite dimensions in the case of E-polarization:

$$h_E(x) = \mathrm{Mod}\,\Sigma(\theta, \vartheta_0)\, e^{i\mathrm{Arg}\,\Sigma(\theta, \vartheta_0)}, \tag{13}$$

By analogy we have for H-polarizatio

$$h_H(x) = \mathrm{Mod}\,\Sigma(\theta, \vartheta_0)\, e^{i\mathrm{Arg}\,\Sigma(\theta, \vartheta_0)}. \tag{14}$$

The x-coordinate on the surface of a radio hologram fixed in some way is related to the angular coordinate θ by the expression

$$\vartheta = \omega x / v_0, \tag{15}$$

where ω is the angular velocity of spin of the object, v_s is the rate of registration of the radio hologram on the recording material.

Reconstruction of the image corresponding to the position of the object at time t = 0 (t ∈ [-T/2, T/2], where T is the interval of synthesis of the radio hologram) reduces to truncated Fourier transformation of the function of the radio hologram [Ref. 4]:

$$V(\omega_x) = \int_{-vT/2}^{vT/2} h(x) e^{i\omega_x x}\, dx, \tag{16}$$

where ω_x is the coordinate in the image space.

The intensity of the image, from which the local scattering characteristics of the object are determined [Ref. 2], is

$$W(\omega_x) = |V(\omega_x)|^2. \tag{17}$$

The algorithm of digital modeling of the radio holographic process reduces to the following procedures based on expressions (13), (14), (16) and (17). Assigned as initial data are the dimensions a and l of the cylinder and wavelength λ. The functions $h_E(\Delta\theta \cdot p)$ and $h_H(\Delta\theta \cdot p)$ are calculated in discrete form, where p is a whole-number parameter that ensures a range of the argument in the interval $0 \leqslant \theta < 2\pi$. The discretization step Δθ is determined in accordance with the theorem of readings from the condition $\Delta\theta \leqslant \lambda/l$. For subsequent processing, readings are selected from the total data file of values of the functions $h_E(\Delta\theta \cdot p)$ and $h_H(\Delta\theta \cdot p)$ that correspond to the angular interval $\theta_H - \Psi_S/2 \leqslant \Delta\theta \cdot p \leqslant \theta_H + \Psi_S/2$, where θ_H is the required radius of observation of the object, $\Psi_S = \omega T$ is the angular size of the radio hologram. The latter has an optimum value [Ref. 3] equal to $\Psi_S = (\lambda/2l)^{1/2}$. The image of the object for aspect θ_H is reconstructed from the corresponding sample by the fast Fourier transform algorithm. In this connection the step of image discretization is equal to $\Delta\omega_x = \lambda/2\Psi_S$. Finally, the images of individual scattering centers are identified with respect to function (17), and the local scattering characteristics are determined.

In Fourier analysis of limited data files, the phenomenon of "blurring" of spectral components arises [Ref. 5], which corresponds to the spectrum of the scattering function of an object with a function of the type sin z/z in the image space. Therefore, instead of a set of δ-functions corresponding in

the limit to the images of the "shining" points, functions of the type $\sin z/z$ arise. The side lobes of these functions cause an error in measurement of the local scattering characteristics that is fundamentally inherent in the given method and restricts its potential accuracy. In other words, the images of the scattering centers are "blurred" by the edge waves that arise at the ends of the hologram. The level of the side lobes can be minimized by apodization, i. e. by multiplying the sample to be processed by a certain weighting function [Ref. 5]. We used two weighting functions in our work:

$$C_1(q)=\begin{cases}\frac{1+\sin[\pi(2Q\cdot q-Q)/2Q]}{2} & \text{for all other } q\end{cases}, \quad q=\overline{1,0,1\cdot Q} \text{ and } q=\overline{0,9\cdot Q,Q}, \tag{18}$$

$$C_2(q)=e^{-3\left(\frac{2q-Q-1}{Q-1}\right)^2}, \tag{19}$$

where q is the ordinal number of the discrete reading, and Q is the volume of the sample to be processed.

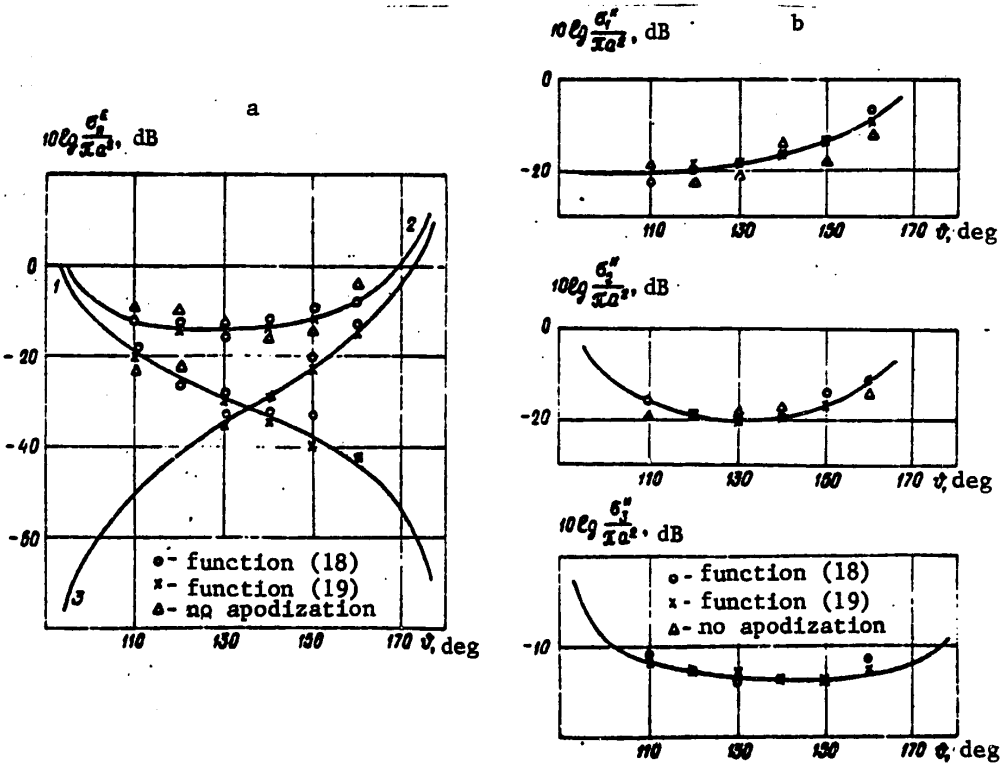

Fig. 2

Fig. 2 shows the results of digital modeling for a cylinder with dimensions $a = 15\lambda$, $l = 4\lambda$ and diagrams of the effective surface scattering of scattering centers of the same object calculated in the single-position case by using

the relations

$$\left.\begin{aligned}\sigma_n^E(\vartheta) &= \pi a^2 |\Sigma_n(\vartheta)|^2 \\ \sigma_n^H(\vartheta) &= \pi a^2 |\Sigma_n(\vartheta)|^2\end{aligned}\right\} n = 1, 2, 3 . \quad (20), (21)$$

Obviously the error of measuring local scattering characteristics that is inherent in the Fourier radio holography method may reach 3-5 dB. Use of weighting functions (18) and (19) can reduce this error to 1 dB and 0.5 dB respectively. Apodization leads to "expansion" of the image of each scattering center, i. e. to deterioration of resolution. For example on Fig. 2a, in the case of using weighting function (19) the values of effective surface scattering of scattering centers 1 and 2 are lacking for certain aspects ($\theta = 110°$, $120°$, $130°$). This is due to the fact that the images of these centers merged into one another. This effect is observed to a lesser extent when weighting function (18) is used. Thus the weighting function for processing radio holograms must be selected from the condition of minimizing the measurement error and maximizing resolution.

These analytical relations were verified experimentally by the method of Fourier radio holograms under conditions of an anechoic chamber. The procedure for conducting the experiment is given in Ref. 2-4. The corresponding part of the modeling algorithm was used for digital reconstruction of images.

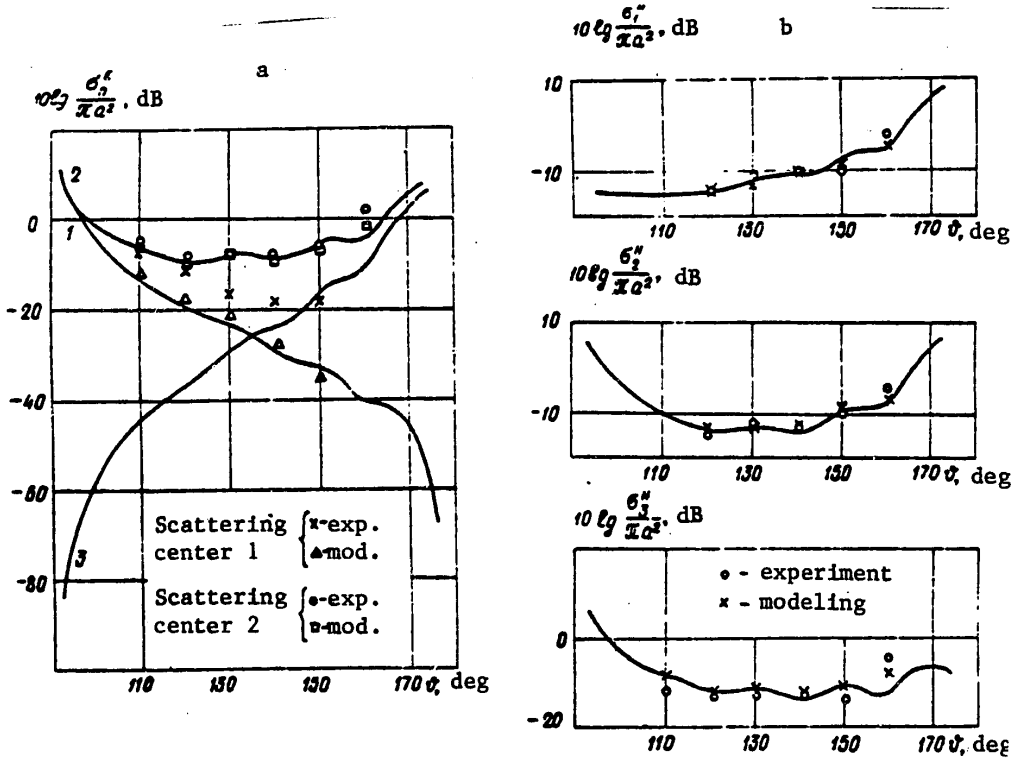

Fig. 3

Fig. 3 shows measured values of local scattering characteristics of an ideally conductive cylinder of length 5λ and radius λ, diagrams of the effective scattering surfaces of scattering centers, and also the results of modeling (using weighting function (19)). The estimate of the rms deviation for the experimental values of the local scattering characteristics was 1.8 dB. In addition to the error of the method itself, which in the given case was 0.5 dB, the overall measurement error includes components due to background reflections in the anechoic chamber, signal fluctuations in the reception and transmitting channels, nonideality of isolation between polarization channels, etc. Thus the error of measurement of local scattering characteristics introduced directly by the experimental facility is approximately 1.3 dB.

For H-polarization (Fig. 3b), the results of theory, modeling and experiment coincide within the limits of the total measurement error. In the case of E-polarization (Fig. 3a), the discrepancy between data of modeling and experiment (especially noticeable for scattering center 1) can apparently be attributed to the approximate nature of the initial formulas. The absence of experimental values of the effective scattering surface of scattering center 3 (Fig. 3a) is due to the fact that the intensity of its image did not exceed the level of the general background.

In summing up, we can draw the following conclusions. For measuring the local scattering characteristics of various objects, it is advisable to use an ideally conductive cylinder of finite dimensions as a reference standard. An edge wave method is used to get analytical expressions for this cylinder that describe its local scattering properties and ensure satisfactory coincidence of theoretical and experimental results. In virtue of the approximate nature of the resultant formulas in the case of E-polarization, only the characteristic of the scattering center situated on the joining between the illuminated end face and lateral surface of the cylinder can be used for referencing. The algorithm developed for digital modeling of the radio holographic process for reference objects enables verification of the efficacy of the measurement facility, evaluation of instrumental error of measurement and the error introduced by the method of Fourier radio holography itself. The potential accuracy of measuring local scattering characteristics can be improved to 0.5 dB by using apodization on the stage of reconstructing the image of the object.

The proposed algorithm can also be used to solve the following problems:

1) determination of the permissible extent of action of various distorting factors on accuracy of measuring local scattering characteristics;

2) selection of optimum parameters for recording radio holograms;

3) investigation of different methods for digital processing of radio holograms for the purpose of correcting and eliminating distortions, improving the signal-to-noise ratio, implementing spatial filtration, etc.

REFERENCES

1. Ufimtsev, P. Ya., "Metod krayevykh voln v fizicheskoy teorii difraktsii" [Edge Wave Method in Physical Diffraction Theory], Moscow, "Sov. radio", 1962.

2. Zinov'yev, Yu. S., Pasmurov, A. Ya. in: "Teoriya difraktsii i rasprostraneniya voln. VII Vsesoyuznyy simpozium po difraktsii i rasprostraneniyu voln, g. Rostov-na-Donu, 1977. Kratkiye teksty dokladov" [Theory of Wave Diffraction and Propagation. Seventh All-Union Symposium on Wave Diffraction and Propagation, Rostov-na-Donu, 1977. Abstracts of Reports], Vol 3, Moscow, 1977, pp 279-282.

3. Popov, S. A., Rozanov, B. A., Zinov'yev, Yu. S., Pasmurov, A. Ya. in: "Materialy VIII Vsesoyuznoy shkoly po golografii" [Materials of the Eighth All-Union School on Holography], Leningrad, 1976, pp 275-297.

4. Zinov'yev, Yu. S., Pasmurov, A. Ya., PIS'MA V ZHURNAL TEKHNICHESKOY FIZIKI, Vol 3, No 1, 1977, pp 28-32.

5. Bergland, G. D., IEEE SPECTRUM, Vol 6, No 7, 1969, pp 41-67.

UDC 621.391.156

FUNCTIONAL CAPABILITIES OF DEVICES WITH OPTICAL FEEDBACK

[Article by V. B. Astaf'yev]

[Text] An examination is made of the functional capabilities of devices with optical feedback. It is shown that the increase of information input to devices with optical feedback that realize transformations in the spatial coordinates of the device is limited by the time required for the optical signal to pass through the optical feedback circuit. A further increase in the rate of information input enables expansion of the functional capabilities of the device with optical feedback by synthesis of an optical digital filter. The weighting coefficients of optical digital filters are functions of two arguments and act on the spatial characteristics of the optical signal propagating in the optical feedback. In this way it becomes possible to process three-dimensional information in which one of the coordinates is time, while the other two correspond to the spatial coordinates of the device.

The development of optical data processing is determined both by the development of an element base of optical computer facilities, and by expansion of the class of optically realizable transformations. Devices with optical feedback have enabled expansion of the algorithmic capabilities of optical processors. Devices with optical feedback can be used to synthesize a real-time amplitude-phase filter [Ref. 1], to synthesize an inverse filter [Ref. 2],

to eliminate multiplicative interference [Ref. 3] and nonlinear transformation of images [Ref. 4], to solve Freholm's integral equations of the first kind by synthesis of Wiener and Tikhonov filters and by the iteration method [Ref. 5-7], and to solve Fredholm's integral equations of the second kind [Ref. 5, 6, 8].

The widespread opinion that the rate of data processing in optical computing devices is limited for practical purposes only by the the time of data input [Ref. 9] is not completely valid in the case of devices with optical feedback at high rates of data input since the time for feeding information into a device with optical feedback may be comparable with the time that the optical information signal is in the device repeatedly passing through the optical feedback circuit; furthermore, delay of the optical information signal in the optical feedback circuit does not lead to simple time shift of the processing result as is the case in devices without optical feedback. Thus in realizing transformations [Ref. 1-8] the time of information input (and thereby the time of transformation) must be greater than the quantity NT, where T is the time required for an optical information signal to pass through the optical feedback circuit, N is the number of passages of the light through the optical feedback circuit that are taken into consideration in synthesizing the transformation; $T = L_{oc}/c$, where L_{oc} is optical length of the optical feedback circuit, c is the speed of light.

On the other hand, in the case of matching the rate of information input to the delay T of the optical signal in the optical feedback circuit, the possibility is opened up for expansion of the functional capabilities of the device by using a time coordinate in addition.

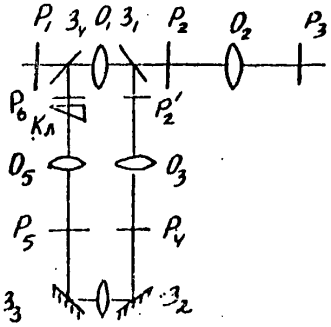

Let us consider the device shown in the diagram, which is analogous to a device with optical wedge in the optical feedback circuit [Ref. 4].

Device with optical feedback: O_1-O_5--Fourier transformation lenses; *Кл*--optical wedge; P_1 and P_3--input and output planes; P_2, P_2', P_3 and P_6-- frequency and object planes respectively

The device is a correlator of diffraction type [Ref. 9] consisting of Fourier transformation lenses O_1 and O_2 with the addition of a feedback circuit formed by mirrors $З_1$, $З_2$, $З_3$, $З_4$ and Fourier transformation lenses O_3, O_4, O_5. Optical wedge *Кл* is introduced in the object plane of the optical feedback circuit to shift the optical beam by an amount $\Delta\omega_x$ in the space frequency plane. A plane-parallel plate inclined to the optical axis and located in the frequency plane of the optical feedback circuit can also be used as an element for shifting the beam by the amount $[\Delta\omega_x]$.

Let the distribution of light in plane P_1 be equal to $S(x, y, t)$, and let the transmission of transparencies be $A_n(\omega_x, \omega_y)$ in plane P_2, and $B_n(\omega_x, \omega_y)$

in plane P_2' or P_5, transparencies $A_n(\cdot,\cdot)$ and $B_n(\cdot,\cdot)$ being localized in the neighborhoods of points $\omega_x = n\Delta\omega_x$ and $\omega_x = (n-1)\Delta\omega_x$ respectively, and being of size $\Delta\omega_x \times \Delta\omega_y$, where $\Delta\omega_x$ and $\Delta\omega_y$ are the dimensions of the spatial spectra of signal S(x, y, t) along coordinates x and y respectively. The transmission of the optical wedge is equal to $\exp(i\Delta\omega_x x)$. Then the distribution of light in the output plane P_3 is equal to

$$S'_{out}(x,y,t) = \sum_{n=0}^{N} \exp(in\Delta\omega_x x)\hat{L}^{(n)} S(x,y,t), \qquad (1)$$

where $\hat{L}^{(n)}$ is an operator equal to

$$\hat{L}^{(n)} = S(x,y,t) \otimes K_n(x,y) \otimes \delta(t-nT) =$$
$$= \int_{-\infty}^{\infty} S(x,y,t) K_n(\xi - x, \eta - y)\delta(\tau - t + nT)\, d\xi\, d\eta\, d\tau,$$

$K_n(x,y)$ is the inverse Fourier transform of function $K_n(\omega_x, \omega_y)$,

$$K_n(\omega_x,\omega_y) = A_n(\omega_x,\omega_y) B_1(\omega_x,\omega_y) B_2(\omega_x,\omega_y) \ldots B_n(\omega_x,\omega_y) =$$
$$= A_n(\omega_x,\omega_y) \prod_{k=1}^{n} B_k(\omega_x,\omega_y).$$

The factor $\exp(in\Delta\omega_x x)$ in (1) arises as a consequence of the optical wedge in the object plane of the optical feedback, and leads to nonlinearity of the optical system as does any transparency in the object plane of the optical feedback circuit [Ref. 4]. Assuming the influence of the phase factor is eliminated by one of the methods given below, (1) is transformed to the following expression:

$$S_{out}(x,y,t) = \sum_{n=0}^{N} \hat{L}^{(n)} S(x,y,t), \qquad (2)$$

that describes a linear system with transfer function

$$K(\omega_x,\omega_y,\omega_t) \sum_{n=0}^{N} K_n(\omega_x,\omega_y) \exp(-i\omega_t nT), \qquad (3)$$

where ω_t is the angular time frequency.

Expression (3) is obtained from (2) by triple Fourier transformation of both sides of the equation with respect to coordinates x, y, t.

Comparing transfer function (3) with the transfer function of an electronic digital filter [Ref. 10], which takes the form

$$K(\omega_t) = \sum_{n=0}^{N} K_n \exp(-i\omega_t nT),$$

we can treat the system with optical feedback as an optical digital filter that is an optical analog of the electronic digital filter, the weighting

coefficients in front of factors exp $(-i\omega_t nT)$ in the optical digital filter, in contrast to the coefficients of the electronic digital filter, being functions of the spatial coordinates ω_x, ω_y.

The analogy between optical and electronic digital filters shows up most completely when

$$\prod_{k=1}^{n} B_k(\omega_x, \omega_y) = \exp(-i\omega_x n x_0).$$

Then

$$K(\omega_x, \omega_y, \omega_t) = \sum_{n=0}^{N} A_n(\omega_x, \omega_y) \exp(-i\omega_x n x_0) \exp(-i\omega_t nT).$$

In this case, the digital filter realizes summation of the weighted signals S(x, y, t) shifted not only with respect to time coordinate by nT, but also with respect to space coordinate by nX_0.

If $\Delta\omega_x = 0$ (no optical wedge in the object plane in the optical feedback circuit), the transfer function of the system takes the form

$$K(\omega_x, \omega_y, \omega_t) = \sum_{n=0}^{\infty} A^n(\omega_x, \omega_y) B^n(\omega_x, \omega_y) \exp(-i\omega_t nT) = \frac{A(\omega_x, \omega_y)}{1 - A(\omega_x, \omega_y) \exp(-i\omega_t T)}. \quad (4)$$

and corresponds to a recursive optical digital filter of first order. Let us take up methods of compensating the phase factor in sum (1). We note that if $\Delta\omega_x = 0$, this problem does not arise.

1. Incoherent summation of luminous fluxes in the output plane [Ref. 4]. In this case the coherence length L_{kor} of the light source must be less than L_{oc}. The class of transformations in spatial coordinates is fairly narrow.

2. Multiplying the spatial spectrum of light distribution in the output plane P_3 with subsequent filtration using a spatial slit filter of size $[-\Delta\omega_x/2, \Delta\omega_x/2]$ by the algorithm

$$S_{6ux}(x,y,t) = \left\{ S'_{6ux}(x,y,t) \sum_{l=0}^{N'} \exp(-il\Delta\omega_x x) \right\} \omega \operatorname{sinc} \frac{\Delta\omega_x}{2} x =$$
$$= \left\{ \sum_{n=0}^{N} \sum_{l=0}^{N'} \exp[i(n-l)\Delta\omega_x x] \hat{L}^{(n)} S'(x,y,t) \right\} \omega \operatorname{sinc} \frac{\Delta\omega_x}{2} x = \sum_{n=0}^{N} \hat{L}^{(n)} S(x,y,t),$$

where $\sum_{l=0}^{N} \exp(-il\Delta\omega_x x)$ is the transmission function of the spatial spectrum multiplier. The condition $L_{kor} > L_{oc}$ must be met.

3. The holographic method of summing light fluxes [Ref. 7]. A special case of the holographic method is heterodyning. By using a device analogous to that in the diagram (p 36) and including a time modulator for shifting the frequency of light by an amount ω_{t_0}, a fan of reference light beams is produced

$$\sum_{n=0}^{N} \exp(in\Delta\omega_x x)\exp(i\omega_{t_0} t), \qquad (5)$$

that are combined with information signal (1), each information light flux appearing in sum (1) corresponding to a reference beam in sum (5) that is collinear and coherent only to that particular flux. Quadratic detection of the output signal at each point of the output plane by a photocell with subsequent electronic filtration of the time signal using a filter with transmission center ω_{t_0} ensures electrical summation of the terms of sum (2). In this case it is necessary that $L_{kor} < L_{oc}$.

The base of the three-dimensional signal to be processed in a device with optical feedback is determined by the product of the signal base with respect to the time coordinate and the signal base with respect to space coordinate. The base of the signal being processed with respect to time coordinate is determined by the number of filters located in plane P_2 and is equal to N+1. Since N+1 and N filters are situated in the respective frequency planes P_2 and P_2' of the device, the information capacity in spatial coordinates of a device with optical feedback is N+1 times less than that of a device without optical feedback. Thus the information capacity with respect to time and space coordinates is redistributed in the device with optical feedback. The quantity N is limited chiefly by losses of light in the optical feedback circuit. Inclusion of an optical wedge in the output plane of the optical feedback circuit enables use of a mirror with reflectivity near 100% as mirror 3_4 by oblique input of the optical beam into the optical feedback circuit [Ref. 4], which considerably reduces light losses. Besides, an active medium can be used for light amplification in the optical feedback circuit [Ref. 2]. In case of necessity, the luminous fluxes that pass through the optical feedback circuit can be equalized in intensity in plane P_2, where N is determined by a reasonable value of efficiency of utilization of the power of the light source.

The time for passage of a light signal through the optical feedback circuit at $L_{oc} = 2$ m, $c = 3\ 10^{[8]}$ m/s, is 6.7 ns, which corresponds to an upper limiting time frequency of the signal introduced into the optical digital filter of 75 MHz, whereas existing electro-optical and acousto-optical light modulators enable data input to optical computers with speeds in excess of 1 GHz.

Thus the time aspect when considering devices with optical feedback is useful since in the first place it enables estimation of the limiting speed of devices with optical feedback that realize transformations in spatial coordinates, and in the second place it opens up the capability for synthesis of optical digital filters that realize transformations of three-dimensional information.

REFERENCES

1. Gallagher, N. C., APPL. OPT., Vol 15, No 4, 1976, p 882.

2. Hagler, M. D., APPL. OPT., Vol 10, No 2, 1971, p 2783.

3. Händler, E., Röder, V., OPT. COMMUNS., Vol 23, No 3, 1977, p 352.

4. Nevezhenko, Ye. S., Sepktor, B. I., AVTOMETRIYA, No 3, 1976, p 98.

5. Astaf'yev, V. B., "Tezisy dokladov II Vsesoyuznoy shkoly po opticheskoy obrabotke informatsii" [Abstracts of Reports to the Second All-Union School on Optical Data Processing], Gor'kiy, 1978, p 36; also in: "Opticheskaya obrabotka informatsii" [Optical Data Processing], collection of papers edited by S. B. Gurevich, Leningrad, 1979, p 139.

6. Vasilenko, G. I., "Teoriya vosstanovleniya signalov" [Theory of Signal Reconstruction], Moscow, "Sov. radio", 1979.

7. Astaf'yev, V. B., "Tezisy dokladov III Vsesoyuznoy shkoly po opticheskoy obrabotki informatsii" [Abstracts of Reports to the Third All-Union School on Optical Data Processing], Riga, 1980, p 116.

8. Auslender, A. L., Vishnyakov, G. N., Levin, G. G., Stepanov, B. M., in: "Opticheskaya obrabotka informatsii", collection of papers edited by S. B. Gurevich, Leningrad, 1979, p 107.

9. Vasilenko, G. I., "Golograficheskoye opoznavaniye obrazov" [Holographic Pattern Recognition], Moscow, "Sov. radio", 1977.

10. Gonorovskiy, I. S., "Radiotekhnicheskiye tsepi i signaly" [Electronic Circuits and Signals], Moscow, "Sov. radio", 1977.

UDC 621.391.14

SIGNAL AND INTERFERENCE AT INPUT OF ACOUSTO-OPTICAL SPECTRUM ANALYZER

[Article by S. V. Kulakov]

[Text] The paper analyzes passage of a normal steady-state random signal and a useful signal through an electro-optical spectrum analyzer.

The acousto-optical spectrum analyzer (Lambert analyzer) is attracting particular attention in connection with the fact that it can be used for real-time processing of radio signals with spectral width of several hundred MHz ("super wide-band signals") on carrier frequencies up to several GHz.

A large number of papers have been devoted to studies of this device, which is shown schematically in Fig. 1. In particular, the following frequency-response function (response to σ-action in the frequency region) was found

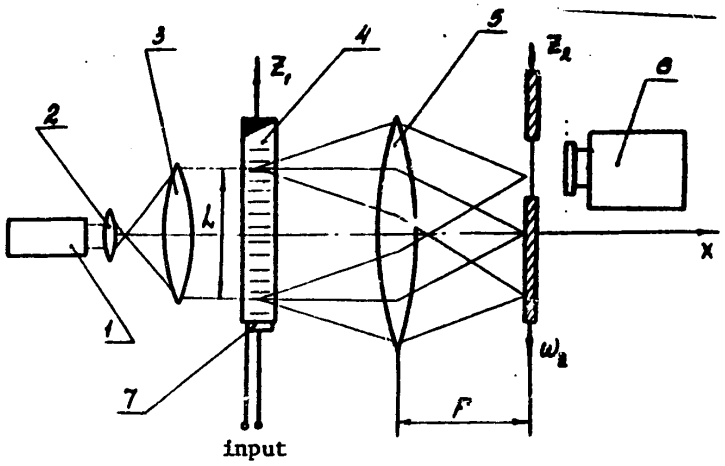

Fig. 1. Schematic diagram of acousto-optical spectrum analyzer: 1--coherent light source; 2--condenser lens; 3--collimator; 4--acoustic light modulator; 5--integrating objective lens; 6--registration device (photodetector); 7--piezoelectric transducer

in Ref. 1, 2:

$$\dot{G}(\omega-\omega_{3\theta},t)=\frac{\sin(\omega-\omega_{3\theta})\frac{T}{2}}{\omega-\omega_{3\theta}}e^{j(\omega-\omega_{3\theta})\frac{T}{2}}e^{-j(\omega-\omega_{3\theta})t}, \qquad (1)$$

where $\omega_{3\theta}$ is the frequency of the harmonic input signal; $T = L/v$ is the duration of the sample being analyzed; L is the dimension of the aperture of the acoustic light modulator in the direction of elastic wave propagation; v is the velocity of the elastic waves in the medium of acousto-optical interaction.

It can be easily demonstrated that when the passband of the acoustic light modulator is limited and the elastic waves are damped in the modulator medium, the frequency-response function is defined by the relation

$$\dot{G}(\omega,\omega_{3\theta},t)=\dot{K}_{\eta}(\omega_{3\theta})e^{-\alpha(\omega_{3\theta})\frac{L}{2}}e^{j(\omega-\omega_{3\theta})\frac{T}{2}}\frac{\mathrm{sh}(\alpha(\omega_{3\theta})v-j(\omega-\omega_{3\theta}))\frac{T}{2}}{(\alpha(\omega_{3\theta})v-j(\omega-\omega_{3\theta}))}e^{-j(\omega-\omega_{3\theta})t} \qquad (2)$$

where $\dot{K}_{\eta}(\omega_{3\theta})$ is the complex transfer constant of the piezoelectric transducer of the acoustic light modulator $\alpha(\omega_{3\theta})$ is the frequency-dependent damping factor of elastic waves in the medium of acousto-optical interaction.

The frequency-response function of the analyzer enables us to find the output spectral distribution in accordance with the expression [Ref. 1, 2]:

$$\dot{S}_{6\omega_x}(\omega,t)=\frac{A_0}{2\pi}\int_{-\infty}^{+\infty}\dot{S}(\omega_{3\theta})\dot{G}(\omega,\omega_{3\theta},t)\,d\omega_{3\theta}, \qquad (3)$$

where $\dot{S}(\omega)$ is the spectrum of an arbitrary input signal; $\dot{S}_{вых}(\omega,t)$ is the instantaneous output spectrum; A_c is the modulation index corresponding to a harmonic input signal of unit amplitude. We will use this defining characteristic of the device to analyze transmission of random signals through it.

For linear systems, including the Lambert analyzer at low input signal level [Ref. 2], the energy spectrum and autocorrelation function of a random input signal are most simply found [Ref. 3, 4].

Let a continuous random steady-state (in the broad sense) ergodic process X(t) with normal distribution law be sent to the input of the device. Its energy spectrum is $W(\omega)$, autocorrelation function -- $\psi(\tau)$, and variance -- σ^2. Let us find analogous characteristics of a random signal in the output plane of the analyzer, i. e. in the spatial frequency plane.

Let us isolate one realization of the random signal $X_i(t)$. Its spectral density is

$$\dot{S}_i(\omega) = \int_{-\infty}^{+\infty} x_i(t) e^{-j\omega t}\, dt . \tag{4}$$

In accordance with (3), the spectral distribution in the output plane of this realization can be written as follows:

$$\dot{S}_{i\,вых}(\omega,t) = \frac{A_0}{2\pi} \int_{-\infty}^{+\infty} \dot{S}_i(\omega_{зв})\, \dot{G}(\omega, \omega_{зв}, t)\, d\omega_{зв} . \tag{5}$$

Relation (5) defines the instantaneous spectrum of realization $X_i(t)$. Here the duration of the sample being analyzed is $T = L/v$. It is obvious that $\dot{S}_{i\,вых}(\omega, t)$ varies in a random way from one realization to another.

Let us find the square of the modulus (5):

$$S_{i\,вых}^2(\omega,t) = \dot{S}_{i\,вых}(\omega,t)\, \dot{S}^*_{i\,вых}(\omega,t) = \frac{A_0^2}{4\pi^2} \int_{-\infty}^{+\infty}\int_{-\infty}^{+\infty} \dot{S}_i(\omega'_{зв})\, \dot{S}^*_i(\omega''_{зв})\, \dot{G}(\omega,\omega'_{зв},t)\, \dot{G}^*(\omega,\omega''_{зв},t)\, d\omega'_{зв}\, d\omega''_{зв} . \tag{6}$$

(Here and below * is the sign of complex conjugation). Let us carry out statistical averaging in (6). In doing this, we consider the fact that operations of integration and averaging are commutative.

Thus we have

$$\langle S_i^2(\omega,t)\rangle = \frac{A_0^2}{4\pi^2 T} \int_{-\infty}^{+\infty}\int_{-\infty}^{+\infty} \langle \dot{S}_i(\omega'_{зв})\, \dot{S}^*_i(\omega''_{зв})\rangle\, \dot{G}(\omega,\omega'_{зв},t)\, \dot{G}^*(\omega,\omega''_{зв},t)\, d\omega'_{зв}\, d\omega''_{зв} \tag{7}$$

(As a consequence of ergodicity of the process, averaging over the set of realizations is replaced in (7) by time averaging within the limits of one realization of duration T). We note than in accordance with Ref. 3 (p 90)

$$\overline{\langle \dot{S}_i(\omega')\,\dot{S}_i^*(\omega'')\rangle} = 2\pi\delta(\omega'-\omega'')W\left(\frac{\omega'+\omega''}{2}\right), \tag{8}$$

where $W(\omega)$ is the energy spectrum of the input signal. Substituting (8) in (7) and carrying out integration over $\omega''_{3\theta}$, we have

$$\begin{aligned}\overline{\langle \dot{S}_{i\,вых}(\omega,t)\rangle} &= \\ &= \frac{A_0^2}{2\pi}\int_{-\infty}^{+\infty} W(\omega_{3\theta})\dot{G}(\omega,\omega_{3\theta},t)\,\dot{G}^*(\omega,\omega_{3\theta},t)\,d\omega_{3\theta} = \\ &= \frac{A_0^2}{2\pi}\int_{-\infty}^{+\infty} W(\omega_{3\theta})\,G^2(\omega,\omega_{3\theta},t)\,d\omega_{3\theta}.\end{aligned} \tag{9}$$

For steady-state processes (9) can be written as

$$\overline{W_{вых}(\omega)} = \frac{A_0^2}{2\pi T}\int_{-\infty}^{+\infty} W(\omega_{3\theta})\,G_1^2(\omega,\omega_{3\theta})\,d\omega_{3\theta}, \tag{10}$$

where $W_{вых}(\omega)$ is the energy spectrum of the random output signal; $\dot{G}_1(\omega, \omega_{3\theta})$ is the aperture-frequency function of the modulator.

The aperture-frequency function is obtained by dropping cofactor $e^{-j(\omega-\omega_{3\theta})t}$ in (2), and it depends on $\alpha(\omega_{3\theta})$, the shape of the aperture of the acoustic light modulator, and the bandwidth of its piezoelectric transducer. For the centered processes with which we are primarily concerned, the variance is

$$\overline{G^2_{вых}} = \frac{1}{2\pi}\int_{-\infty}^{+\infty} W_{вых}(\omega)\,d\omega. \tag{11}$$

Thus (9), (10) and (11) define the statistical characteristics of a random spatial signal in the output plane of the analyzer. Since this is a linear device, when the input process is normal, the output signal will also have normal distribution. The autocorrelation function of the output signal in accordance with the Wiener-Khinchin theorem will be defined by the Fourier transform of (10). In this operation, it is necessary to convert to spatial frequencies ω_z by the substitution [Ref. 2] $\omega = \omega_z v$.

Let us now find the signal-to-noise ratio in the output plane of the analyzer and at the output of the photodetector. Each point of this plane situated on the spatial frequency axis can be treated as an individual optical output of the device, while the photodetector (see Fig. 1) transforms the optical output signal to an electric signal.

Let us assume that a photodiode matrix is used as the photodetector. Such extraction of the optical output distribution can be used in analyzing periodic signals or signals with slowly changing spectra.

When photodiodes are used to transform the optical output signal to an electric signal, linear detection of the modulated luminous flux takes place.

Thus the electric output signal is proportional to the square of the amplitude of the light wave at a given point in the output plane. Here the meaning of "point in the output plane" is arbitrary since the luminous flux to one element of the photodiode matrix emanates from some small area. However, this "point" concept can be used if the size of such an area on the spatial frequency axis does not exceed the extent of one element of resolution $\Delta f_p = 1/T$. The number N of elements of resolution is usually determined from the relation

$$N = 2\Delta f \cdot T = \frac{2\Delta f}{\Delta f_p} \quad , \tag{12}$$

where $2\Delta f_0$ is the band of simultaneous analysis.

The useful signal at the j-th point of the plane is determined by the harmonic component of the input signal of frequency ω_j. Interference at this point depends on the component of the random signal at the input of form

$$U_j(t) = V_j(t)\cos(\omega_j t + \varphi_j(t)) \quad , \tag{13}$$

where $A_j(t)$ and $\phi_j(t)$ are random processes with distribution laws that in the general case are different from normal.

Thus the signal-to-noise ratio at the j-th point of the output plane of the analyzer and also on its j-th electric output can be obtained by examining the transmission of an additive mixture of useful harmonic signal and a random signal of type (13) through the device, i. e. the signal

$$e_s(t) = U_j(t) + V_c \cos\omega_j t \quad . \tag{14}$$

We disregard the set noises of the analyzer, assuming that conditions are met that appreciably reduce their level [Ref. 5]. Let us assume that the interference at the input of the device is a steady-state random ergodic process with normal distribution law, and $W(\omega)$, $\psi(\tau)$ and σ_x^2.

Let us also assume that signal (13) is likewise a normal steady-state ergodic process [Ref. 4]. At a low level of signal (13), we get narrow-band random light fluctuations of frequency $\omega_{CB} + \omega_j$ (or $\omega_{CB} - \omega_j$) also with a normal distribution law (ω_{CB} is the light frequency of the coherent light source). Let us determine the variance σ_j^2 of these oscillations. In virtue of additivity of the variances of components of the random spatial signal in the output plane of the analyzer, finite resolution, and a limited number of elements of resolution of the analyzer, we can write

$$\sigma_{вых}^2 = \sigma_1^2 + \sigma_2^2 + \ldots + \sigma_N^2 = \sum_{j=1}^{N} \sigma_j^2 \tag{15}$$

where

$$\sigma_j^2 = \frac{1}{2\pi} W_{вых}(\omega_j) \frac{2\Delta\omega_0}{N} \quad , \tag{16}$$

and $2\Delta\omega_0 = 2\pi 2\Delta f_0$.

Considering (12), we have

$$\sigma_j^2 = W_{вых}(\omega_j)\Delta f_p = W_{вых}(\omega_j)\frac{1}{T} \tag{17}$$

The mean square of the envelope of the random signal at the j-th point [Ref. 4] is

$$\langle A_j^2 \rangle = 2\sigma_j^2 \tag{18}$$

The amplitude of the useful signal at this point of the output plane in accordance with (13) is determined by the relation

$$A_{j0} = A_0 U_c \frac{1}{2\pi}\int_{-\infty}^{+\infty} \pi\delta(\omega-\omega_j)\dot{\sigma}(\omega,\omega_j,t)\,d\omega = A_0\frac{U_c}{2}\sigma_i(\omega_j,\omega_j). \tag{19}$$

Thus the signal-to-noise ratio (with respect to power) at the output of the i-th photodetector can be written in the following form:

$$\frac{A_{j0}^2}{2\sigma_j^2} = \frac{\pi}{4\Delta f_p^2}\,\frac{U_c^2\,\sigma_i^2(\omega_j,\omega_j)}{\int_{-\infty}^{\infty} W(\omega)\,\sigma_i^2(\omega_j,\omega)\,d\omega}. \tag{20}$$

Relation (20) shows that when the resolution of the analyzer is increased, there is an increase in the signal-to-noise ratio at its output. Such a conclusion is readily explained. Actually, the higher the resolution of the device, the more "narrow-banded" is each of its outputs. And in narrow-band systems it is easier to isolate the signal from the band noise.

It can be readily shown that in the case of white noise ($W(\omega) = W_0$), relation (20) easily reduces to the form

$$\frac{A_{j0}^2}{2\sigma_j^2} = \frac{\frac{U_c^2}{2}T}{W_0} = \frac{\mathcal{E}}{W_0}, \tag{21}$$

where $\mathcal{E}$ is the energy of a radio pulse of duration T, i. e. of the sample of the harmonic input signal determined by the dimensions of the aperture of the acoustic light modulator.

Now let us find the signal-to-noise ratio at the output of the photodetector. To do this, it is necessary to consider the action on the quadratic photodetector by an additive mixture of harmonic signal and narrow-band noise, i. e. a signal of the form

$$U_\phi(t) = A_{j0}\cos(\omega_{cc}+\omega_j)t + A_j(t)\cos\left((\omega_{cc}+\omega)t + \varphi_j(t)\right). \tag{22}$$

An analogous problem was solved for example in Ref. 4 (see p 422). We will use the results obtained there.

The variance of the output process is

$$\sigma_{j\,вых}^2 = \Phi_0^2\left(A_{j0}^2\sigma_j^2 + \sigma_j^4\right), \tag{23}$$

where Φ_0 is a parameter that accounts for the properties of the photodetector and the characteristics of the low-frequency filter that acts as the load.

The useful signal is

$$U_c = \Phi_0 \frac{A_{j0}^2}{2} \tag{24}$$

The signal-to-noise ratio at the output of the photodetector is

$$\frac{U_c}{\sigma_{j\,ш}} = \frac{\frac{A_{j0}^2}{2\sigma_j^2}}{\sqrt{1+2\frac{A_{j0}^2}{2\sigma_j^2}}} . \tag{25}$$

Substituting (20) in (25) we get relations for calculating the signal-to-noise ratio on the j-th output of the analyzer.

Let us note that at low signal-to-noise ratios [Ref. 4]

$$\frac{U_c}{\sigma_{j\,ш}} \approx \frac{A_{j0}^2}{2\sigma_j^2} , \tag{26}$$

and at high ratios

$$\frac{U_c}{\sigma_{j\,ш}} \approx \frac{1}{2}\frac{A_{j0}^2}{2\sigma_j^2} . \tag{27}$$

In the case of white noise at the input of the spectrum analyzer, the variance of the random signal in the band of analysis $2\Delta\omega_0$ is determined by the relation

$$\sigma_{вх}^2 = 2\Delta f_0 W_0 . \tag{28}$$

Then the signal-to-noise ratio (with respect to power) at the input of the analyzer can be written in the following form:

$$\frac{U_c^2}{2\sigma_{ш}^2} = \frac{U_c^2}{4\Delta f_0 W_0} . \tag{29}$$

Consequently

$$\frac{\frac{A_{j0}^2}{2\sigma_j^2}}{\frac{U_c^2}{2\sigma_{ш}^2}} = 2\Delta f_0 T = N \tag{30}$$

Thus the "narrow-band filtration" that occurs in the spectrum analyzer leads to improvement of the signal-to-noise ratio at a given point of the output plane by a factor equal to the number of elements of resolution of the device.

REFERENCES

1. Kulakov, S. V., Moskalets, O. D., Razzhivin, B. P., "Some Questions in the Theory of the Optical-Acoustic Spectrum Analyzer", TRUDY LENINGRADSKOGO INSTITUTA AVIATSIONNOGO PRIBOROSTROYENIYA, No 64, 1969, pp 96-108.

2. Kulakov, S. V., "Akustoopticheskiye ustroystva spektral'nogo i korrelyatsionnogo analiza signalov" [Acousto-Optical Devices for Spectral and Correlation Analysis of Signals], Leningrad, "Nauka", 1978.

3. Tikhonov, V. I., "Statisticheskaya radiotekhnika" [Statistical Electronics], Moscow, "Sov. radio", 1966.

4. Gonorovskiy, I. S., "Radiotekhnicheskiye tsepi i signaly" [Electronic Circuits and Signals], Moscow, Sov. radio", 1977.

5. Preston, K., "Kogerentnyye opticheskiye vychislitel'nyye mashiny" [Coherent Optical Computers], Moscow, "Mir", 1974.

UDC 621.317

FREQUENCY-RESPONSE FUNCTION OF REAL ACOUSTO-OPTICAL SPECTRUM ANALYZER

[Article by V. V. Molotok]

[Text] The paper examines operation of an acousto-optical spectrum analyzer with consideration of oblique incidence of a plane light wave on a light modulator, attenuation and diffraction divergence of the elastic wave.

The principal comprehensive characteristic of a spectrum analyzer as a linear device is its frequency-response function [Ref. 1], i. e. the response to a δ-action in the frequency plane, which corresponds to harmonic oscillation of unit amplitude. The input and output of a linear instrument are related by the superposition integral, which for the case of a spectral instrument is written:

$$\dot{S}_2(\omega) = \int_{-\infty}^{\infty} \dot{S}_1(\omega')\,\dot{g}(\omega, \omega')\,d\omega',$$

where $\dot{g}(\omega, \omega')$ is the frequency-response function, $\dot{S}_1$, $\dot{S}_2(\omega)$ are spectral distributions at the input and output of the spectrum analyzer. The frequency-response function of an ideal acousto-optical analyzer is described in Ref. 2, and takes the form:

$$g_0(f, f', t) = \frac{\sin[\pi(f-f')T]}{\pi(f-f')T} \exp[j2\pi f'(t-0{,}5T)],$$

where T is the duration of time sampling. This paper examines only interaction of a plane light wave and an undamped non-diverging elastic wave for Raman-Nath or Bragg diffraction conditions. In real acousto-optical spectrum

analyzers that have a band of analyzable frequencies of up to several hundred megahertz, spectrum reproduction is influenced by absorption and diffraction divergence of the elastic wave. In this connection, we can no longer speak of a pure Bragg or Raman-Nath diffraction mode since the angle of incidence of the plane light wave on the light modulator is adjusted to get a predetermined band of analysis. Therefore we would like to get an expression for the frequency-response function of an acousto-optical spectrum analyzer considering the influence that diffraction divergence and attenuation of elastic waves as well as oblique incidence of a plane light wave have on the light modulator.

An optical diagram of an acousto-optical spectrum analyzer with arbitrary incidence of a plane light wave on the light modulator is shown in Fig. 1.

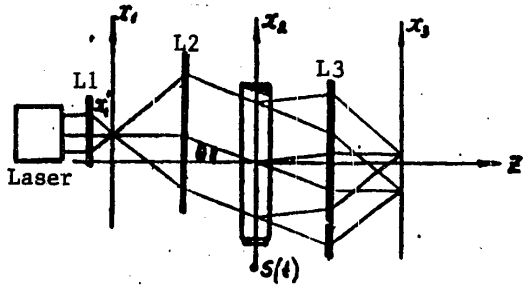

Fig. 1

In the front focal plane of the collimating lens (plane x_1) is a point light source $e(t, x_1) = (x_1 - x_1') \exp(j\omega_{C\theta} t)$, where $\omega_{C\theta}$ is the frequency of the light waveforms. The light signals in the rear focal plane of the collimating lens (plane x_2) are defined by

$$e(t, x_2) = \int_{-\infty}^{\infty} e(t, x_1) \exp\left(j \frac{2\pi}{\lambda F} x_1 x_2\right) dx_1 = \exp(j\omega_{C\theta} t) \exp\left(j \frac{2\pi}{\lambda F} x_2 \frac{x'}{F}\right),$$

where λ is the wavelength of light, F is the focal length of the collimating lens. Then the light wave incident on the light modulator can be written as

$$e(t, x_2, z) = \exp\left[j(\omega_{C\theta} t + \frac{2\pi}{\lambda} x_2 \operatorname{tg}\theta - K_{C\theta} z)\right] = \exp\left[j K_{C\theta} (ct + x_2 \operatorname{tg}\theta - z)\right],$$

where c and $K_{C\theta}$ are the speed of propagation and wave number of the light wave, θ is the angle between the direction of the z-axis and the normal to the wavefront of the light wave incident on the modulator. That is, a plane light wave is incident on the light modulator at angle θ. This wave is modulated by an elastic wave propagating in the medium of interaction, that is excited by a piezoelectric transducer upon transmission of an electric waveform. For determining the frequency-response function, such a waveform is a harmonic signal of unit amplitude, and an elastic wave

$$S(t, x_2) = \sin\left[\omega' t - \kappa'(x_2 - 0,5L)\right],$$

propagates in the medium of interaction of light and sound, where L = v·T; v and K' = ω'/v are the velocity of propagation in the medium of interaction and the wave number of the elastic wave. The light wave in the output plane of the light modulator that forms the first diffraction order is defined as

$$\dot{e}_{+1}(t, x, z) = H(K', \theta) \exp\left\{ j\left[(\omega_{cs} t + K_{cs} x_2 \operatorname{tg}\theta - K_{cs} z) + (\omega' t - K' x_2 + 0{,}5 K' l)\right]\right\},$$

where H(K', θ) is a weighting function that accounts for the geometry of interaction of light and sound. The weighting function H(K', θ) describes the amplitude-frequency response of acousto-optical interaction independently of the mode of diffraction, and is defined as [Ref. 3]:

$$H(K', \theta) = \frac{\sin\left[\frac{K'}{\cos\theta}\left(\sin\theta + 0{,}5\frac{K'}{K_{cs}}\right) 0{,}5 l\right]}{\frac{K'}{\cos\theta}\left(\sin\theta + 0{,}5\frac{K'}{K_{cs}}\right) 0{,}5 l} \exp\left[j \frac{K'}{\cos\theta}\left(\sin\theta + 0{,}5\frac{K'}{K_{cs}}\right) z \right],$$

where l is the interaction length of light and sound. The light waveforms in the output plane of the spectrum analyzer (plane x_3) are defined as the Fourier transform of luminous distribution in plane x_2, i. e. the light signals in the output plane of the spectrum analyzer in the vicinity of the first diffraction order are defined as

$$\dot{e}_{+1}(t, x_3) = \int_{-0{,}5L}^{0{,}5L} \dot{e}_{+1}(t, x_2) \exp\left(j \frac{2\pi}{\Lambda F} x_2 x_3 \right) dx_2 =$$

$$= \exp\left\{ j\left[\omega_{cs} t - (\omega_1 + \omega_3)(t + 0{,}5T)\right]\right\} \cdot \frac{vT}{l} H(K', \theta) \dot{g}_0(\omega_1, \omega_3, \omega', t),$$

where $\dot{g}_0(\omega_1, \omega_3, \omega', t)$ is the frequency-response function of an ideal acousto-optical spectrum analyzer. Thus the frequency-response function of an acousto-optical spectrum analyzer with consideration of oblique incidence of a plane light wave on the light modulator is defined as

$$\dot{g}_1(\omega_1, \omega_3, \omega', t) = H(K', \theta) \dot{g}_0(\omega_1, \omega_3, \omega', t).$$

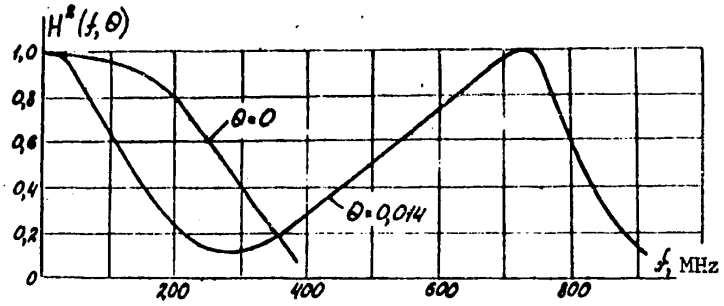

Fig. 2

Fig. 2 shows the results of calculation of the amplitude-frequency response of acousto-optical interaction for different angles of incidence of a plane

light wave on the light modulator where the material of the interaction medium is $LiNbO_3$ ($\ell = 2$ mm, $v = 6.57 \cdot 10^6$ mm/s, $n_0 = 2.2$).

An examination is made in Ref. 4 of the influence that damping of elastic waves in the material of the medium of interaction of light and sound has on the frequency-response function of an acousto-optical spectrum analyzer, i. e. the case is considered in which the elastic wave

$$S(t, x_2) = \exp[-\alpha(\omega'_x)(x_2 + 0{,}5L)]\sin[\omega' t - \omega'_x(x_2 + 0{,}5L)]$$

propagates in the interaction medium, where $\alpha(\omega'_x)$ is the coefficient of damping of elastic waves in the material of the interaction medium, $\omega'_x = \omega'/v$ is spatial frequency, $0.5L \leqslant x_2 \leqslant 0.5L$ [sic]. The frequency-response function of the acousto-optical spectrum analyzer with consideration of damping of elastic waves in the material of the interaction medium is defined by

$$\dot{g}_2(\omega, \omega', t) = \exp[-0{,}5\alpha(\omega'_x)L]\frac{\operatorname{sh}\{0{,}5[\alpha(\omega'_x) + j(\omega_x + \omega'_x)]L\}}{0{,}5[\alpha(\omega'_x) + j(\omega_x + \omega'_x)]L}\exp[-j(0{,}5\omega_x L - \omega' t)]$$

Considering that over a broad frequency range the absorption of elastic waves in solids is a square-law function of frequency, i. e. $\alpha(\omega'_x) = \Gamma f'^2$, the frequency-response function of an acousto-optical spectrum analyzer can be written as

$$\dot{g}_2(f, f', t) = \exp[-0{,}5\Gamma v T f'^2]\frac{\operatorname{sh}[0{,}5\Gamma v T f'^2 - j\pi(f - f')T]}{0{,}5\Gamma v T f'^2 - j\pi(f - f')T}\exp[j2\pi f'(t - 0{,}5T)].$$

In the case of small elastic wave damping, i. e. $0.5\Gamma v T f'^2 \to 0$, the expression for the frequency-response function with consideration of damping is written as

$$\dot{g}'_2(f, f', t) = 0{,}5[1 + \exp(-\Gamma v T f'^2)]\,\dot{g}_2(f, f', t).$$

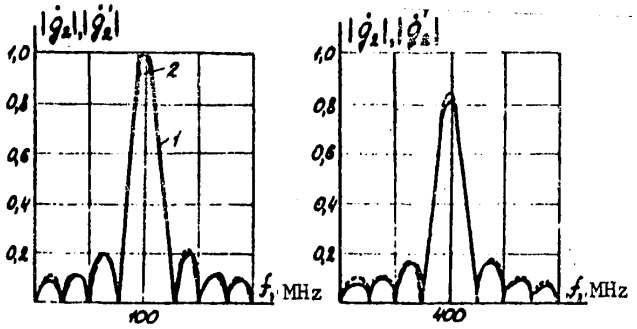

Fig. 3

Fig. 3 shows the results of calculation of the frequency-response function of an acousto-optical light analyzer with consideration of damping of elastic waves by exact and approximate formulas (curves 1 and 2 respectively). The material of the interaction medium was $PbMoO_4$ ($T = 5$ μs, $v = 3.75 \cdot 10^6$ mm/s, $\Gamma = 11.5$ dB/cm GHz^2).

In considering the diffraction divergence of the elastic waves, it is assumed that $\ell > h$, where $\ell \times h$ is the area of the transducer. In this case the elastic wave can be considered divergent only with respect to the dimension h of the piezoelectric transducer. Then a wave

$$S(t,x,y) = A(x,y)\sin[\omega' t - \kappa' x + \varphi(x,y)]$$

propagates in the material of interaction of light and sound (Fig. 4), where A(x, y), ϕ(x, y) are the amplitude and phase of the wave excited in the interaction medium when a harmonic waveform of unit amplitude with frequency ω' is applied.

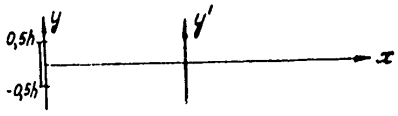

Fig. 4

To determine the amplitude and phase of the wave, we consider oscillations (pressure change in the interaction medium). Perturbations of the interaction medium caused by the transducer can be defined as [Ref. 5]:

$$f(x,y') = \frac{1}{\sqrt{\lambda x}} \int_{-\infty}^{\infty} f(y)\exp\left[j\frac{\kappa'(y'-y)^2}{2x}\right] dy,$$

where λ is the wavelength of the elastic wave, f(y) is the pressure distribution over the transducer. We assume that pressure distribution over the transducer is uniform, i. e.

$$f(y) = \begin{cases} 1, & |y| \le \frac{h}{2}; \\ 0, & |y| > \frac{h}{2}. \end{cases}$$

then

$$f(x,y') = \frac{1}{\sqrt{\lambda x}} \int_{-h/2}^{h/2} \exp\left[j\frac{\kappa'(y'-y)^2}{2x}\right] dy =$$

$$= \frac{1}{\sqrt{2}}\left\{[C(\tau_N) - C(\tau_0)] + j[S(\tau_N) - S(\tau_0)]\right\} = \frac{1}{\sqrt{2}} A(x,y')\exp[j\varphi(x,y')],$$

where

$$\tau_N = \sqrt{\frac{2}{\lambda x}}\left(y' + \frac{h}{2}\right); \qquad \tau_0 = \sqrt{\frac{2}{\lambda x}}\left(y' - \frac{h}{2}\right);$$

$C(z) = \int_0^z \cos\left(\frac{\pi x^2}{2}\right) dx$ is the Fresnel cosine integral;

$S(z) = \int_0^z \sin\left(\frac{\pi x^2}{2}\right) dx$ is the Fresnel sine integral;

$$A(x,y') = \left\{[C(\tau_N) - C(\tau_0)]^2 + [S(\tau_N) - S(\tau_0)]^2\right\}^{\frac{1}{2}}; \quad \varphi(x,y') = \operatorname{arctg}\left[\frac{S(\tau_N) - S(\tau_0)}{C(\tau_N) - C(\tau_0)}\right]$$

The given elastic wave interacts with the plane light wave incident on the light modulator. The light signals in the output plane of the spectrum analyzer in the region of first diffraction order are defined by

$$e_{+1}(\omega_x, \omega_y, t) = \exp[j(\omega_{cs} + \omega')t] \int_0^L \int_{-0,5h}^{0,5h} A(x,y') \exp[j\Psi(x,y')] \cdot$$

$$\cdot \exp[j(\omega_x - K')x] \cdot \exp(j\omega_y \cdot y')\,dx \cdot dy'.$$

This expression defines the frequency-response function of the acousto-optical spectrum analyzer with consideration of the diffraction divergence of elastic waves. Direct calculation of the function from the derived formula involves calculation of triple integrals since the amplitude and phase of the elastic wave are determined by Fresnel integrals. Therefore to reduce the multiplicity of the integration we use a representation of Fresnel integrals in the form of sums [Ref. 6]:

$$S(x) = \begin{cases} 0, & |x| \le 0,15; \\ S\sqrt{\frac{2}{\pi z}}\left(\frac{3\sin z}{z^3} - \frac{3\cos z}{z^2} - \frac{\sin z}{z}\right), & 0,15 < |x| \le 1,25; \\ 0,5 - \frac{\cos z}{\sqrt{2\pi z}}, & |x| > 1,25, \end{cases}$$

$$C(x) = \begin{cases} 0,5 + \frac{\sin z}{\sqrt{2\pi z}}, & |x| \ge 1,25, \text{ where } z = \frac{\pi x^2}{2}; \\ \frac{6}{\sqrt{2\pi z}}\left(\frac{\sin z}{2z} - \frac{\cos z}{z}\right), & |x| < 1,25. \end{cases}$$

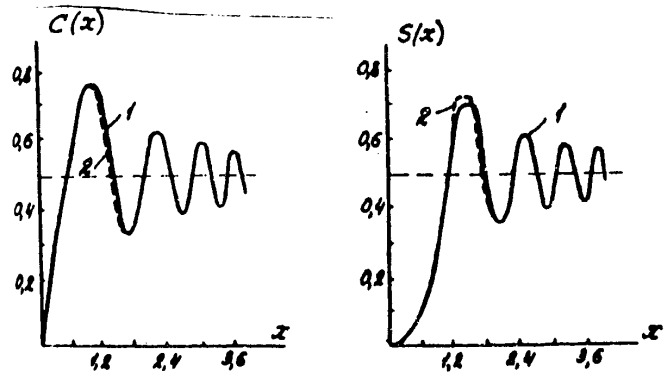

Fig. 5

For negative values of x: $c(-x) = -c(x)$; $s(-x) = -s(x)$. Fig. 5 shows the results of calculation of Fresnel integrals by the exact formula (curve 1) and by the approximate formula (curve 2).

REFERENCES

1. Khurgin, Ya. I., Yakovlev, V. P., "Finitnyye funktsii v fizike i tekhnike" [Finite Functions in Physics and Engineering], Moscow, "Nauka", 1971.

2. Kulakov, S. V., "Akustoopticheskiye ustroystva spektral'nogo i korrelyatsionnogo analiza signalov" [Acousto-Optic Devices for Spectral and Correlation Analysis of Signals], Leningrad, "Nauka", 1978.

3. Cohen, M. G., Gordon, E. J., "Acoustic Beam Probing Using Optical Techniques", THE BELL SYSTEM TECHNICAL JOURNAL, April 1965, pp 693-721.

4. Molotok, V. V., Razzhivin, V. P., "Influence of Acoustic Wave Damping on the Characteristics of Acousto-Optical Spectrum Analyzers" in: "Akustoopticheskiye metody i tekhnika obrabotki informatsii" [Acousto-Optic Methods and Data Processing Techniques], Leningrad, 1980.

5. Papulis, A., "Teoriya sistem i preobrazovaniy v optike" [Theory of Systems and Transformations in Optics], Moscow, "Mir", 1971.

6. Abramovits, M., Stigan, I. M., editors, "Spravochnik po spetsial'nym funktsiyam" [Handbook on Special Functions], "Nauka", 1979.

UDC 621.396:535.8

STATISTICAL CHARACTERISTICS OF ACOUSTO-OPTIC RECEIVERS OF LONG PSEUDORANDOM SIGNALS

[Article by A. V. Kuzichkin]

[Text] An examination is made of the problem of finding pseudo-random signals from code sequence delay by using a system comprising an acousto-optic convolver and recirculation delay line. Expressions are obtained for the probability of correct determination of the time position of a pseudo-random signal and the average duration of the signal detection procedure for the case of reception against a background of white gaussian noise. It is assumed that the duration of the received signal considerably exceeds the time of signal delay in the region of acousto-optical interaction of the acousto-optic convolver.

Correlation reception of pseudo-random signals is one of the most promising areas for using acousto-optical processors. The interest that has arisen in the design of pseudo-random signal receivers based on acousto-optical processing systems can be attributed primarily to the comparative simplicity of realization by using algorithms of matched filtration of pseudo-random signals under conditions of considerable uncertainty in the time position of signals to be received. From the standpoint of maximizing flexibility in adaptation of receivers to changing conditions of pseudo-random signal reception, it is advisable to make the processing system in an acousto-optic

convolver arrangement [Ref. 1] in which the processing algorithm is restructured by changing the law of formation of the reference signal.

In the general case, the acousto-optic convolver is not a processor that is invariant to the time position of the signal to be processed. However, if the duration of the received signal does not exceed the time of delay (T_3) of the signal in the region of acousto-optical interaction of the acousto-optic convolver, then determination of the time of pseudo-random signal arrival can be ensured for practical purposes within a single reception cycle at the expense of slightly increased complexity of the receiver and the use of continuous-wave transmission of the reference signal. Unfortunately in most actual cases the pseudo-random signal duration is considerably greater than time T_3. To eliminate the energy losses that arise when processing such signals in an acousto-optic convolver, the output responses of the convolver are accumulated by using recirculation delay lines [Ref. 2] or photo-CCD's [Ref. 3]. As a result, the acousto-optic receiver loses the capacity for searchless determination of pseudo-random signal arrival time, and requires the use of special synchronization procedures [Ref. 4].

This paper evaluates the statistical characteristics of procedures of pseudo-random signal search and processing by using an acousto-optical receiver consisting of an acousto-optic convolver and recirculation delay line. A block

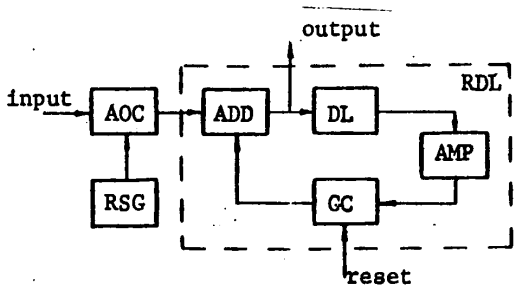

Fig. 1

diagram of the device to be analyzed is shown in Fig. 1, where RSG is the reference signal generator, ADD is an adder, DL is a delay line, AMP is an amplifier, GC is a gating circuit that cuts off accumulation of the output signal of the acousto-optic convolver [AOC, and RDL is the recirculation delay line]. The choice of the recirculation delay line as a cumulative element is dictated by the fact that in many cases the use of a recirculation delay line gives the required accumulation interval (up to a few milliseconds), and realization of an acousto-optic receiver with recirculation storage is far simpler than for a receiver with photo-CCD storage.

In the most general case, the procedure of searching for pseudo-random signals by using an acousto-optic convolver with recirculation delay line consists in sequential step-by-step correlation analysis of the signal being received at different delays of the reference signal. The decision on detection of a

acousto-optic convolver is made with respect to the maximum output signal of the recirculation delay line after analyzing the entire region of temporal uncertainty of the signal being received.

Evaluation of the statistical characteristics of pseudo-random signal detection by an acousto-optic receiver of the given type will be based on the following quite general assumptions.

1. The size of the region of acousto-optical interaction of the convolver is selected in such a way that a whole number of recirculation cycles $R = T_c/T_3$ is required for processing a pseudo-random signal of duration T_c.

2. The signal arriving at the receiver input is formed by pseudo-random signal repetition formed in accordance with a law of the same pseudo-random sequence.

3. The reference signal sent to the acousto-optic convolver is formed by breaking down the initial pseudo-random signal into [missing letter] segments of duration T_3 each, and by time inversion of the resultant segments.

4. The beginning of the recirculation period coincides with the beginning of the first segment of the reference pseudo-random signal.

Let us use the symbol ΔT to denote the time mismatch between the beginning of the received pseudo-random signal and the beginning of the reference pseudo-random signal. In doing this, we will assume that if the input signal leads the reference signal, $\Delta T < 0$, while if the input signal lags, $\Delta T > 0$ ($|\Delta T| \leq T_c/2$).

We can readily see that the output correlation peak of the recirculation delay line and the time of its appearance are linearly dependent on the instantaneous value of ΔT, and are determined by expressions of the form

$$J = c_0(1 - |\Delta T|/2T_3) \; ; \tag{1}$$

$$\Delta t = T_3 - \Delta T/2 \; , \tag{2}$$

where c_0 is a proportionality constant and Δt is the interval between the beginning of the reference signal and the occurrence of the correlation peak.

The principal characteristics of a correlation receiver operating in the mode of pseudo-random signal search are mean duration of the signal detection procedure ($\overline{T_0}$) and probability of correct determination of its time position (P_{np}). We will find these characteristics for the most typical case of incoherent reception of pseudo-random signals against a background of gaussian white noise with zero average and correlation function of the form $\frac{1}{2}N_0\delta(t_2-t_1)$.

The average time of pseudo-random signal detection by the algorithm considered in this paper will be found as

$$\overline{T_0} = T_c P_{np} + 2T_c(1 - P_{np})P_{np} + \ldots + kT_c(1-P_{np})^{k-1}P_{np} = T_c/P_{np} \; , \; k = \overline{1,\infty}. \tag{3}$$

Here T_a is the duration of the procedure of analyzing the output signal of the recirculation delay line in investigation of the entire region of temporal uncertainty of the pseudo-random signal being received. The quantity T_a is determined by the duration of the received signal, the time of delay of the signal in the acousto-optic convolver, the number of recirculation cycles required and the search step ΔT_m (i. e. the time shift of the reference signal of the acousto-optic convolver in step-by-step examination of the zone of possible time position of the pseudo-random signal):

$$T_a = T_c T_3 R/\Delta T_m .$$

In this paper the statistical values are analyzed for two values of the search step: $\Delta T_{m1} = T_3$ and $\Delta T_{m2} = 2T_3$. The selection of just these values of ΔT_m is dictated by the following factors.

1. To get correlation peaks at the output of the recirculation delay line with amplitude at any initial temporal mismatch ΔT that would be sufficient for comparatively successful detection of pseudo-random signals against a background of intense noises, relation (1) tells us that the condition

$$\Delta T_m \leqslant 2T_3$$

must be met.

2. Displacement of the reference signal by an amount that is a multiple of T_3 considerably simplifies realization of a tunable reference pseudo-random signal generator and a generator control system.

In the case of search for signals with step $\Delta T_{m1} = T_3$, the procedure for analysis of the output signal of the recirculation delay line takes up time interval $T_{a1} = T_c R$, and in searching for the time position of the pseudo-random signal with step $\Delta T_{m2} = 2T_3$, the duration of the analysis procedure is equal to $T_{a2} = T_c R/2$. In the case of search with step T_3 for analysis time T_{a1}, four signal correlation peaks will be observed at the output of the recirculation delay line, whereas there will be only two correlation peaks in the case of search with step $2T_3$ for analysis time T_{a2}. The occurrence of such a number of correlation peaks is due to the fact that for the given search steps the temporal mismatch between the received and reference signals falls within the principal correlation region given by (1) ($|\Delta T| \leqslant 2T_3$) several times (four times for $\Delta T_{m1} = T_3$ and twice for $\Delta T_{m2} = 2T_3$). Then since the time position of the signal being received can be determined from the time of occurrence of any signal correlation peak, probability P_{np} is found as the probability of detecting at least one correlation peak:

$$P_{np1} = 1 - \prod_{i=1}^{4} (1 - P_i) ; \quad (4)$$

$$P_{np2} = 1 - \prod_{i=1}^{2} (1 - P_i) , \quad (5)$$

where P_i is the probability that the amplitude J of the signal correlation peak is greater than amplitude Z of all noise spikes at the output of the recirculation delay line.

In the case of incoherent reception of a pseudo-random signal

$$P_i = \int_0^\infty \omega_1(J)\left[\int_0^J \omega_1(Z)\,dZ\right]^M dJ, \qquad (6)$$

where

$$\omega_1(J) = \frac{J}{h_0^2}\exp\left(-\frac{J^2+h_0^2}{2h_0^2}\right) I_0(J);$$

$$\omega_1(Z) = \frac{Z}{h_0^2}\exp\left(-\frac{Z^2}{2h_0^2}\right);$$

M is the total number of noise spikes ($M = Б - 4$ for ΔT_{m1} and $M = Б - 2$ for ΔT_{m2}); Б is the base of the pseudo-random signal; $h_0^2 = 2E_n/N_0$; E_n is the energy of the signal that yields a correlation peak of magnitude J at the output of the recirculation delay line; $I_0(\cdot)$ is a modified Bessel function of the first kind of zero order.

Transforming expression (6) by a technique such as that described in Ref. 5, we finally get

$$P_i = \int_0^\infty u\exp\left[-(u^2+h_0^2)/2\right] I_0(h_0 u)\left[1-e^{-u^2/2}\right]^M du, \qquad (7)$$

where $u = J/h_0$.

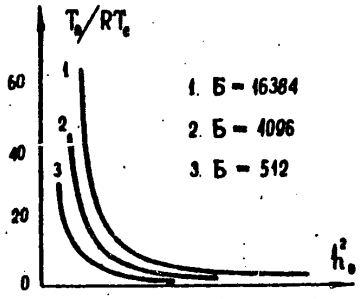

Fig. 2

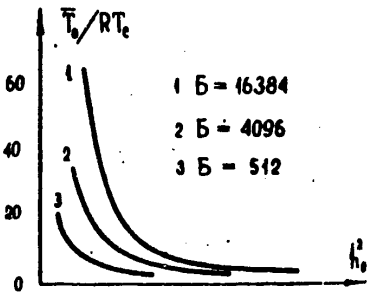

Fig. 3

Fig. 2 and 3 show the average time of pseudo-random signal detection as a function of the signal-to-noise ratio h_0^2 for different values of the base of the pseudo-random signal with maximum mismatch between the received and reference signals. The curves on Fig. 2 are plotted for a search step $T_э$, and on Fig. 3 for a search step $2T_э$. Fig. 4 and 5 show the way that $\bar{T}_0$ depends on h_0^2 at large excesses of the signal over noise (1. Б = 4096, $\Delta T_{m1} = 2T_э$; 2. Б = 4096, $\Delta T_{m1} = T_э$; 3. Б = 512, $\Delta T_{m1} = 2T_э$; 4. Б = 512, $\Delta T_{m1} = T_э$; 5. Б = 16384, $\Delta T_{m1} = T_э$; 6. Б = 16384, $\Delta T_{m2} = 2T_э$). All calculations were done by formula (3) with consideration of relations (4), (5) and (6). Analysis of the resultant curves shows that at comparatively low values of h_0^2 ($\leqslant$10-15) the

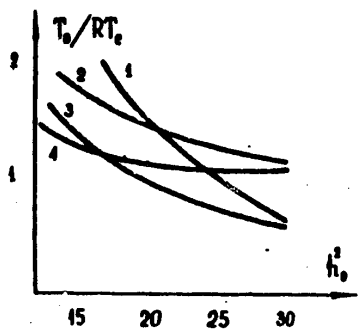

Fig. 4

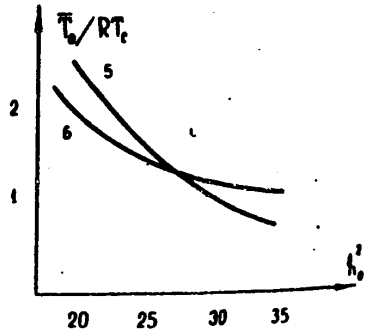

Fig. 5

greatest rate of search of pseudo-random signals is reached at a search step equal to T_3. In the case of signal reception at weak noise levels ($h_0^2 \geqslant 20$) it is advisable to use search with a step $2T_3$ for rapid determination of the time position of pseudo-random signals. The mean duration of the procedure for pseudo-random signal detection is close to $RT_c/2$ in this case, which is B/R times faster then for the case of search using conventional correlation receivers [Ref. 6].

REFERENCES

1. Kulakov, S. V., "Akustoopticheskiye ustroystva spektral'nogo i korrelyatsionnogo analiza signalov" [Acousto-Optic Device for Spectral and Correlation Analysis of Signals], Leningrad, "Nauka", 1978.

2. Morgan, D. P., Hannah, J. M., "Surface Wave Recirculation Loops for Signal Processing", IEEE TRANS. SONICS AND ULTRASONICS, Vol 25, No 1, 1978, p 30.

3. Sprague, R. A., Koliopoulos, K. L., "Time Integrating Acousto-Optic Correlator", APPL. OPTICS, Vol 15, 1976, p 80.

4. Kuzichkin, A. V., "Optical Processing of Complex Signals With Unknown Time Position" in: "Tezisy dokladov III Vsesoyuznoy shkoly po opticheskoy obrabotke informatsii" [Abstracts of Reports to the Third All-Union School on Optical Data Processing], Riga, Part 1, 1980, p 135.

5. Viterbi, E. D., "Printsipy kogerentnoy svyazi" [Principles of Coherent Communications], "Sov. radio", 1970.

6. Tuzov, G. I., "Statisticheskaya teoriya priyema slozhnykh signalov" [Statistical Theory of Complex Signal Reception], Moscow, "Sov. radio", 1977.

UDC 621.396:535.8

ACOUSTO-OPTIC CORRELATION ANALYSIS OF COMPLEX SIGNALS WITH JUMPING FREQUENCY

[Article by A. V. Kuzichkin]

[Text] A method is proposed and analyzed for constructing acousto-optic correlation analyzers that enable determination of the arrival time and carrier frequency of complex signals with jumping frequency practically within the limits of a single reception cycle.

The solution of many problems in present-day electronics involves correlation analysis of signals of complex shape. The use of conventional methods of acousto-optic data processing [Ref. 1, 2] enables correlation analysis only when the carrier frequencies of received and reference signals coincide, which considerably complicates processing of signals produced by combining pseudo-random modulation and stepwise change of carrier frequency [Ref. 3]. The case of frequency uncertainty of the received signal necessitates either considerable complication of the acousto-optic analysis system, using a large number of processing channels with different reference signal carrier frequencies, or else considerable time expenditures on determining the program for tuning the received signal.

In the simplest case, rapid correlation analysis of signals with jumping frequency can be realized by repeatedly shifting the spatial carrier frequency of the reference signal fed to the input of an acousto-optic convolver, which in virtue of its advantages [Ref. 1] is the main element for acousto-optical processing of complex signals. The necessary displacement of the carrier frequency of the reference signal is most simply accomplished by an optical deflector placed in front of an acousto-optic modulator with reference signal to change the angle of incidence of light on the modulator. A considerable disadvantage of such a processing algorithm is the difficulty of realization when searching for signals with a large number of possible values of the carrier frequency. Since the spatial frequency of the reference signal must vary over the entire range of frequency uncertainty of the received signal within a time interval equal to the duration of a single symbol of a pseudo-random sequency of the complex signal*, presently unattainable requirements are imposed on the number of positions of the optical deflector and on the switching speed: in the case of discrete tuning of the carrier frequency of the reference signal, the required speed W_1 for switching the optical deflector, and its capacity E_1 (the number of deflection positions that are resolvable for the Rayleigh criterion) are defined by expressions of the form

$$W_1 = N_f / \tau_0 \quad ; \quad E_1 = N_f \, , \tag{1}$$

*Only in this case can we get simultaneous coincidence of received and reference signals with respect to frequency and delay of the pseudo-random sequence, and consequently only in this case will a correlation peak of maximum possible amplitude be obtained at the output of the acousto-optic processing system for any values of the time and frequency mismatch between the received and reference signals.

where N_f is the total number of possible frequency positions of the received signal, and τ_0 is the duration of one symbol of the pseudo-random sequence.

The requirements for E_1 can be considerably relaxed for example by ensuring repeated coincidence of the received and reference signals with respect to delay of the pseudo-random sequence during propagation of one period of the received signal in the region of acousto-optic interaction of the convolver (T_3). In this case the initial region of frequency search is broken down into m segments (m is the necessary number of coincidences of the received and reference signals with respect to delay of the pseudo-random sequence for time T_3), each of which is analyzed in different time intervals of duration T_3/m. The requirements for parameters of an optical deflector that realizes such series-parallel search for the carrier frequency of received signals are defined by the following relations:

$$\overline{W_2} = N_f/\tau_0 \quad ; \quad E_2 = N_f/m \,, \tag{2}$$

showing a reduction in the necessary capacity of the deflector by a factor m.

The capability of getting repeated coincidence of one period of the received and reference signals with respect to delay of the pseudo-random sequence is implied by the theorem on displcement from the theory of Fourier transforms [Ref. 4]:

$$\mathcal{F}\left\{f(t-t_0)\right\} = F(\omega)\exp(-j\omega t_0) \,, \tag{3}$$

where F is the operator of Fourier transformation.

The output electric signal formed at the output of the photodetector of the acousto-optic analysis system in an acousto-optic convolver arrangement [Ref. 1] is obtained by inverse Fourier transformation of the product of the spatial spectra of the received signal $F_n(\omega-\omega_n)$ and reference signal $F_0(\omega-\omega_0)$:

$$I_{conv}(t) = \mathcal{F}^{-1}\left\{F_n(\omega-\omega_n)\,F_0(\omega-\omega_0)\right\} \,, \tag{4}$$

where ω_n, ω_0 are the angular carrier frequencies of the received signal and the reference signal respectively, and relation (4) is one of the possible forms of writing the field of uncertainty of the complex signal [Ref. 5]:

$$I_{conv}(t) = \chi(\Delta T, \Delta\omega) = \mathcal{F}^{-1}\left\{F_n(\omega-\Delta\omega)F_0(\omega)e^{j\omega\Delta T}\right\} \,. \tag{5}$$

If the spatial spectrum of the received signal is phase-modulated in accordance with (3)

$$F_n(\omega-\omega_n)e^{-j\varphi(t)\omega} \,, \tag{6}$$

and the spatial spectrum of the reference signal is discretely shifted in frequency

$$F_0\left[(\omega-\omega_0)-\Delta\omega_n(t)\right] \,,$$

then the output signal of the processing system will be defined by an expression of the following form:

$$I_{вых}(t) = \chi\left[\Delta T - \alpha(t),\ \Delta\omega - \Delta\omega_M(t)\right],$$

where $\alpha(t)$ is the law of phase modulation of the received signal spectrum; $\Delta\omega_M(t)$ is the law of frequency modulation of the reference signal.

By appropriate selection of the modulation laws $\Delta\omega_M(t)$ and $\alpha(t)$, we can make the output signal of the acousto-optic convolver proportional to the sought correlation function

$$I_{вых}(t) = R\left[\Delta T - \alpha(t)\right] \text{ when } \Delta\omega = \Delta\omega_M(t).$$

Consequently, at the time when $\alpha(t) = \Delta T$, a correlation peak of maximum amplitude will be formed at the output of the acousto-optic analysis system. One of the possible versions of variation of $\Delta\omega_M(t)$ and $\alpha(t)$ is shown in the diagram, where $\Delta\tau_m$, $\Delta\omega_m$ are respectively the greatest time and frequency mismatch

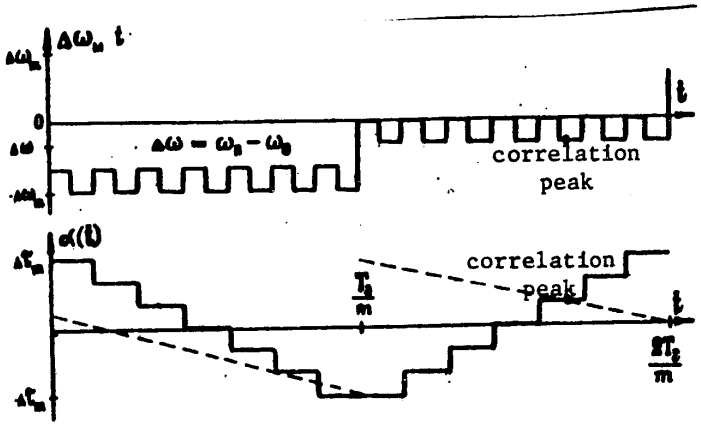

between the received and reference signals, and the broken line shows the current value of time mismatch that varies due to the movement of acoustic waves in the acoustic light modulator, the dot denoting the instant of formation of the maximum correlation peak.

The phase modulation (6) that is necessary for implementing the given algorithm can be realized by using an optical deflector placed in the region of the spatial spectrum of the received signal. In the case of discrete phase modulation of the received signal spectrum, the speed and capacity of this optical deflector are defined by a relation of the form

$$W_0 = m/\tau_0, \quad F_0 = B, \tag{7}$$

where B is the base of the complex signal.

Thus, if $B \ll N_f$ (a condition that is met as a rule when signals with stepwise variation of the carrier frequency are used), with proper choice of the parameter m

$$m_{opt} = N_s/B$$

we can considerably relax the requirements for capacity of optical deflectors that are used without increasing requirements for maximum speed:

$$W_{E\,opt} = N_s/\tau_0 \quad ; \quad W_{S\,opt} = N_s/B\tau_0 \quad : \quad E_{s\,opt} = E_s = B.$$

REFERENCES

1. Kulakov, S. V. "Akustoopticheskiye ustroystva spektral'nogo i korrelyatsionnogo analiza signalov" [Acousto-Optic Devices for Spectral and Correlation Analysis of Signals], Leningrad, "Nauka", 1978.

2. Krupitskiy, E. I., Yakovlev, V. I., "Akustoopticheskiye protsessory radiosignalov" [Acousto-Optic Radio Signal Processors], in: "Akustoopticheskiye metody obrabotki informatsii" [Acousto-Optic Data Processing Methods], Leningrad, "Nauka", 1978, pp 30-45.

3. Dikson, R. K., "Shirokopolyusnyye sistemy" [Wide-Band Systems], Moscow, "Svyaz'", 1979.

4. Goodman, J., "Vvedeniye v Fur'ye-optiku" [Introduction to Fourier Optics], Moscow, "Mir", 1970.

5. Sloka, V. K., "Voprosy obrabotki radiolokatsionnykh signalov" [Problems of Radar Signal Processing], Moscow, "Sov. radio", 1970.

UDC 621.376.2.:535.42

ACOUSTO-OPTICAL RADIO SIGNAL DEMODULATION

[Article by Yu. G. Vasil'yev]

[Text] The paper describes an acousto-optic method of demodulating amplitude-modulated (AM) signals. A method of perturbation theory is used to solve the problem of light diffraction by a complex AM signal when light is obliquely incident on an ultrasonic column. Expressions are derived for distribution of the light field in the region of acousto-optic interaction, and for the intensity of the diffracted light in the spatial frequency plane. Computer-calculated curves are given for the amplitude distortions of the light field as a function of the radio signal frequency bandwidth, as well as the results of an experimental study of an acousto-optical AM signal demodulator working in the Bragg diffraction mode.

Acousto-optical methods are currently being used extensively for radio signal processing. They are used for spectral and correlation analysis [Ref. 1], filtration [Ref. 2] and time scale variation [Ref. 3, 4]. Acousto-optical devices are also known for demodulating frequency-modulated (FM) signals [Ref. 5, 6] that demodulate signals of unit amplitude. However, the need arises in

some processing problems for isolating laws of amplitude modulation (AM) of wide-band radio signals. Besides, when a collimated luminous flux is diffracted by a complex signal, amplitude distortions of the space-time spectrum arise that are due to frequency selectivity of Bragg diffraction. It is necessary to account for such distortions for selecting the frequency band of the linear mode of demodulation.

Let us consider diffraction of a plane light wave

$$E(x,z,t) = C_0 \exp\left\{j\left[k(x\sin\varphi + z\cos\varphi) - \omega_c t\right]\right\}$$

by a phase diffraction grating excited by an AM-FM radio signal in the acousto-optical demodulation system depicted in Fig. 1

$$s(t) = A(t)\cos\left\{2\pi\left[f_0 t + \psi(t)\right]\right\}. \qquad (1)$$

Here C_0 is the amplitude of the light; $k = \omega_c/c$ is the wave number of the light; c is the speed of light in vacuum; ω_c is the cyclic frequency of the light; f_0 is the carrier frequency of the radio signal; $2\pi\psi(t)$ is the slowly varying part of the signal phase.

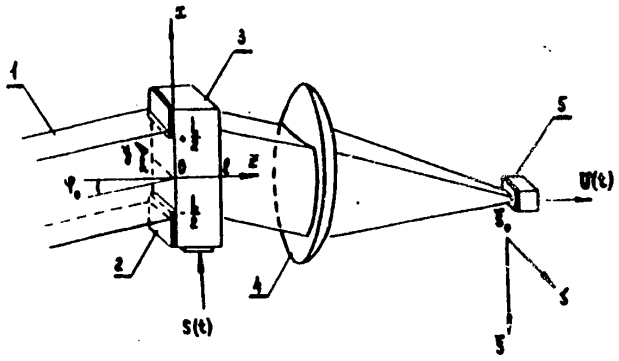

Fig. 1. Acousto-optical demodulation system: 1--luminous flux; 2--aperture diaphragm; 3--ultrasonic light modulator; 4--Fourier lens; 5--photocell

The distribution of light along the cross section of the ultrasonic column in direction Oy is taken as constant and equal to unity in the interval $0 \leqslant y \leqslant h$, where h is the dimension of the ultrasonic column in direction Oy.

Since the frequency of light ($\omega_c/2\pi$) considerably exceeds the frequency $f(t) = f_0 + \psi(t)$ of the radio signal, we can limit ourselves to the quasi-steady case in solving the diffraction problem [Ref. 7].

Distribution of the index of refraction of the acoustic line of the ultrasonic light modulator is described by the relation

$$n(x,t) = n_0\left[1 + \gamma s(x,t)\right].$$

where n_0 is the index of refraction of the unperturbed medium; $\gamma = (\Delta n/n_0)$ is the relative change in amplitude Δn of the index of refraction of the disturbed mdeium;

$$s(x,t) = A(x,t)\cos\left\{2\pi\left[f_0\left(t-\frac{T}{2}-\frac{x}{v}\right)+\psi(x,t)\right]\right\},$$

$T = l/v$ is a time sample corresponding to the working aperture of the acoustic line of the ultrasonic light modulator; v is the velocity of propagation of ultra-sound.

When the quasi-harmonic condition

$$\left|\psi''\left(t-\frac{T}{2}\right)\right|\left(\frac{T}{2}\right)^2 < 0{,}5 \tag{2}$$

and the inequality

$$\frac{T}{2}\left|A'\left(t-\frac{T}{2}\right)\right| \ll \left|A\left(t-\frac{T}{2}\right)\right| \tag{3}$$

are satisfied, the amplitude A(x, t) and phase ψ(x, t) of the ultrasonic wave can be respectively represented in the form

$$A(x,t) \approx A\left(t-\frac{x}{v}\right),$$
$$\psi(x,t) \approx \psi\left(t-\frac{x}{v}\right) - \psi'\left(t-\frac{x}{v}\right).$$

Conditions (2, 3) mean that within the limits of the aperture

$$l < v\left[\frac{2}{\left|\psi''\left(t-\frac{T}{2}\right)\right|}\right]$$

a quasi-harmonic ultrasonic wave propagates with frequency that varies with elapsed time t according to the law

$$f(t) = f_0 + \psi'(t).$$

The amplitude A(x, t) of the wave is a slowly changing function within the limits of the working aperture of the ultrasonic light modulator.

Taking our lead from Ref. 7, let us determine the spectral component E(u, p) of the light field in the region of acousto-optical interaction that is described by the equation

$$\frac{\partial^2}{\partial p^2}E(u,p) + p\frac{\partial^2}{\partial u^2}E(u,p) + \left[1 + 2\gamma A\left(t-\frac{T}{2}\right)\cos u\right]E(u,p) = 0 \tag{4}$$

and boundary conditions of continuity on the media interfaces:

$$E(u,-0) = E(u,+0),$$
$$E(u,kl-0) = E(u,kl+0), \tag{5}$$

where $p = kz$; $u = K(t)x$; $\beta = [K(t)/k]^2$; $K(t) = \frac{2\pi}{v}[f_0 + \psi'(t - \frac{T}{2})]$ is the wave number of the ultrasonic wave.

It is convenient to seek the solution of equation (4) in the form of a seires with respect to powers of γ:

$$E(u,p) = \left[C_0 + \gamma C_1(u,p) + \gamma^2 C_2(u,p) + \cdots\right] \exp\left[j\left(p\cos\varphi + \frac{u\sin\varphi}{\sqrt{\beta}}\right)\right]. \qquad (6)$$

Let us limit ourselves to the function $C_1(u, p)$ that describes the first diffraction orders. We seek the solution in the form

$$C_1(u,p) = B_{+1}(u,p)\exp(-ju) + B_{-1}(u,p)\exp(ju), \qquad (7)$$

where the $B_{\pm 1}(u, p)$ are components of the amplitude of the light wave that forms the first diffraction orders.

Substituting expression (7) in (6) and then in equation (4) with boundary conditions (5), we get the following expression for the coefficients:

$$B_{\pm 1}(x,z,t) = jC_0 A(t-\tfrac{T}{2})\frac{kz}{2\cos\varphi}\,\mathrm{sinc}\left\{\left[\frac{K(t)}{k} \mp 2\sin\varphi\right]K(t)\frac{z}{2\cos\varphi}\right\}\exp\left\{-j\left[\frac{K(t)}{k} \mp 2\sin\varphi\right]K(t)\frac{z}{2\cos\varphi}\right\},$$

where $\mathrm{sinc}\, u = \sin \pi u/\pi u$.

Then light field $E_{+1}(x, \ell, t)$ that arises in the plus of the first diffraction order is described in the region of acousto-optic interaction at $z = \ell$ by the expression

$$E_{+1}(x,\ell,t) = \gamma B_{+1}(x,\ell,t)\exp[-j\Phi(t)]\exp\left\{j\left[kx\left(\sin\varphi - \frac{K(t)}{k}\right)\right]\right\},$$

where $\Phi(t) = \omega_c t - 2\pi\left[f_0(t-\frac{T}{2}) + \psi(t-\frac{T}{2})\right] - \ell\cos\varphi$.

Considering that light distribution along the y-coordinate is constant, we can represent field $E_{+1}(x, \ell, y, t)$ in the form

$$E_{+1}(x,\ell,y,t) = g(y)E_{+1}(x,\ell,t),$$

where

$$g(y) = \begin{cases} 1, & 0 \le y \le h \\ 0, & y < 0 \quad y > h. \end{cases}$$

If the Bragg condition

$$\sin\varphi_0 = \frac{\lambda}{2v}f_0$$

is satisfied for carrier frequency f_0, then intensity $I_{+1}(\xi, \zeta, t)$ of the diffracted light in plane (ξ, ζ) of spatial frequencies of the Fourier lens takes the form

$$I_{+1}(\xi,\zeta,t) = WG(t)A^2(t-\tfrac{T}{2})\,\mathrm{sinc}^2\left\{\frac{L}{\lambda F}\left[\xi - x_0 - \frac{\lambda}{v}F\psi'(t-\tfrac{T}{2})\right]\right\}\mathrm{sinc}^2\left(\frac{h}{\lambda F}\zeta\right), \qquad (8)$$

where $W = (\pi\gamma VC_0/\lambda^2 F)^2$, $V = l\ell h$ is the volume of the region of acousto-optic interaction; F is the focal length of the Fourier lens; λ is the wavelength of the light incident on the ultrasonic light modulator;

$$G(t) = \operatorname{sinc}^2\left\{\frac{Q}{2\pi}\alpha(t)\left[1+\alpha(t)\right]\right\}.$$

$\alpha(t) = [\psi'(t-\frac{T}{2})/f_0]$ is the relative change in frequency of radio signal (1); $Q = (\pi\lambda\ell/\Lambda_0^2)$ is the wave parameter; $\Lambda_0 = v/f_0$ is the wavelength of ultrasound.

It can be seen from expression (8) that the intensity amplitude is proportional to the square of the envelope of the AM-FM signal $A(t-\frac{1}{2}T)$ except for a factor

$$W\,G(t)\operatorname{sinc}^2\left\{\frac{L}{\lambda F}\left[\xi-\xi_0-\frac{\lambda}{v}F\psi'(t-\frac{T}{2})\right]\right\}\operatorname{sinc}^2\left(\frac{\ell}{\lambda F}\eta\right),$$

where G(t) describes distortions that arise due to violation of the Bragg condition on frequencies $f(t) \neq f_0$.

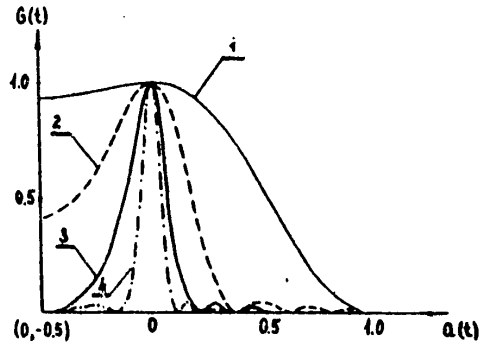

Fig. 2. 1--$Q = \pi$; 2--$Q = 4\pi$; 3--$Q = 8\pi$; 4--$Q = 16\pi$

Curves for G(t) as a function of the relative frequency change $\alpha(t)$ for different values of Q calculated on a BESM-4M computer are shown in Fig. 2.

It can be shown that the frequency band $\Delta\psi'$ in which the relative change G(t) does not exceed 5% of the maximum of its value G(t) = 1 is defined by the formula

$$\Delta\psi' = f_0\left(\sqrt{1+\frac{3{,}13}{Q}}-1\right).$$

If the function $\psi'(t)$ of signal frequency change satisfies the inequality

$$|\psi'(t)| < \frac{\Delta\psi'}{2},$$

then we can set $G(t) \cong 1$ in expression (8) with accuracy to 5%.

The voltage of the electric signal coming from the photocell (see Fig. 1) with center of the photocathode situated at point (ξ_0, 0) is determined from the formula

$$U(t) = \frac{DR}{\Delta\Delta_1}\int_{\xi_0-\frac{\Delta}{2}}^{\xi_0+\frac{\Delta}{2}}\int_{-\frac{\Delta_1}{2}}^{\frac{\Delta_1}{2}} I_{\text{эл}}(\xi,\zeta,t)\,d\zeta\,d\xi \quad , \tag{9}$$

where D is a constant that depends on the photocathode material; R is the load resistance of the photocell; Δ, Δ_1 are the dimensions of the photocathode in directions $O\xi$ and $O\zeta$ respectively.

Omitting intermediate calculations, we get from formula (9)

$$U'(t) = MA^2\left(t-\frac{T}{2}\right)\left\{\text{Si}\left[2\pi b(t)\right] - \frac{\sin^2[\pi b(t)]}{[\pi b(t)]} - \text{Si}\left[2\pi b(t) - 2\pi\frac{\Delta}{d}\right] + \frac{\sin^2\left[\pi b(t) - \pi\frac{\Delta}{d}\right]}{\left[\pi b(t) - \pi\frac{\Delta}{d}\right]}\right\} ,$$

where $U'(t) = (\pi U(t)\Delta\Delta_1/WDRdd_1)$ is the relative change in voltage;

$$M = \text{Si}\left(\pi\frac{\Delta_1}{d_1}\right) - \frac{\sin^2\left(0.5\pi\frac{\Delta_1}{d_1}\right)}{\left(0.5\pi\frac{\Delta_1}{d_1}\right)};$$

Si z is the integral sine; $b(t) = T\psi'\left(t-\frac{T}{2}\right) + \frac{\Delta}{2d}$; $d = (\lambda F/l)$, $d_1 = (\lambda F/h)$ are the dimensions of the light field along $O\xi$ and $O\zeta$ respectively.

If

$$\Delta = \frac{\lambda}{2\psi}f_0\psi' + 4d \quad ,$$

then the output voltage

$$U'(t) \approx \pi M A^2\left(t-\frac{T}{2}\right)$$

is identical to the square of the signal envelope (1).

The given method of acousto-optical demodulation was experimentally verified on a pilot model of an acousto-optic demodulator. The LG-78 laser was used as the light source. The acoustic line of the ultrasonic light modulator was made from a crystal of lithium niobate $LiNbO_3$; the piezoelectric transducer was a plate of lithium niobate $LiNbO_3$ (Y + 36°). The ultrasonic light modulator operated on a frequency of f_0 = 100 MHz in the passband of 20 MHz. The luminous flux was focused by a Fourier lens with focal length of f = 200 mm, and converted to an electric signal by an FD-21KP photocell.

To check the efficacy of the demodulator, an AM-FM signal was used with duration of τ = 10 μs with sinusoidal frequency modulation:

$$f(t) = f_0 + \Delta f \sin(2\pi f_1 t) ,$$

where $f_0 = 100$ MHz, $\Delta f = 1$ MHz, $f_1 = 0.25$ MHz.

Oscillograms of input and output signals are shown on Fig. 3, 4.

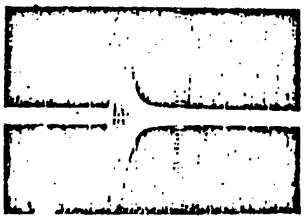

Fig. 3. Input signal

Fig. 4. Output signal

The described acousto-optic method of demodulating complex amplitude-modulated signals enables us to distinguish laws of amplitude modulation of both cw and pulse signals. In addition, the technique enables us to measure time intervals such as signal duration and recurrence period. The results of this paper can be also be used in calculating the geometry of acousto-optic interaction in acousto-optic devices for complex signal processing.

REFERENCES

1. Kulakov, S. V., "Akustoopticheskiye ustroystva spektral'nogo i korrelyatsionnogo analiza signalov" [Acousto-Optic Devices for Spectral and Correlation Analysis of Signals], Leningrad, "Nauka", 1978.

2. Catrona, Leith, Palermo, Parcello, "Optical Systems for Signal Filtration and Processing", ZARUBEZHNAYA RADIOELEKTRONIKA, No 10, 1962.

3. Kulakov, S. V., Kludzin, V. V., Yezhov, V. I., "Acousto-Optic Time Scale Converters" in "Golografiya i obrabotka informatsii" [Holography and Data Processing], Leningrad, "Nauka", 1976.

4. Shulz, M. B., Holland, M. G., Davis, "Optical Pulse Compression Using Bragg Scattering by Ultrasonic Waves", APPL. PHYS. LETT., Vol 11, No 7, 1967.

5. Yegorov, Yu. V., Naumov, K. P., "Acousto-Optic Demodulator of Frequency-Modulated Signals" in "Voprosy analiza i sinteza radiosignalov i ikh obrabotka" [Problems of Analyzing, Synthesizing and Processing Radio Signals], interinstitutional anthology, RRI, LETI, MAI, NPI, No 1, 1976.

6. Vasil'yev, Yu. G., Karpov, Yu. S., Smirnov, L. I., "Optico-Acoustic FM Signal Demodulator", TEKHNIKA SREDSTV SVYAZI, SERIYA OT, No 4(13), 1978.

7. Rytov, S. M., "Light Diffraction by Ultrasonic Waves", IZVESTIYA AKADEMII NAUK SSSR: SERIYA FIZICHESKAYA, No 2, 1937.

UDC 535.42

PECULIARITIES OF LIGHT DIFFRACTION BY COMPLEX ULTRASONIC SIGNALS

[Article by Yu. G. Vasil'yev]

[Text] A solution is found for the problem of light diffraction by a wide-band ultrasonic signal with arbitrary phase function. Computer plots are given of distortions of the diffracted light as a function of width of the signal passband and wave parameter $Q = \pi\lambda\ell/\Lambda_0^2$, where ℓ is the acousto-optical interaction length, λ is the wavelength of light, $\Lambda_0 = v/f_0$ is the wavelength of ultrasound on carrier frequency f_0, v is the velocity of propagation of ultrasound. An expression is derived for calculating optimum length ℓ.

In Ref. 1-3 an investigation is made of the diffraction of coherent light by an ultrasonic harmonic wave. The problem of light diffraction by an ultrasonic wave with linear frequency modulation is fairly well covered for cases of collimated [Ref. 4, 5] and divergent [Ref. 5, 6] light beams. Diffraction by a complex ultrasonic signal with arbitrary phase function is described in Ref. 7, 8. However, the results found there are either applicable to the case [Ref. 7] of a quasi-monochromatic wave $(\Delta\omega/\omega_0) \ll 1$, where $\Delta\omega$, ω_0 are the cyclic width of the frequency band and the carrier frequency respectively, or else are quite cumbersome and require considerable expenditures of computer time in calculations [Ref. 8]. Besides, in solving some applied problems, such as when designing acousto-optic devices, the necessity arises for evaluating distortions of the diffracted light field. Such calculations have not been done up to the present for the case of interaction of light with an ultrasonic signal having a phase function of arbitrary shape.

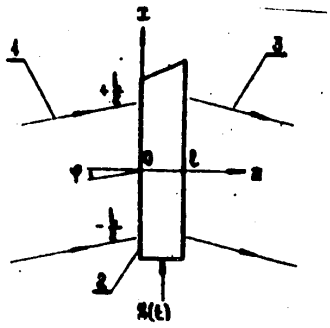

Fig. 1

Acousto-optic system 1--incident light wave; 2--acoustic line, 3--diffracted light

The problem of diffraction of a plane light wave by ultrasound excited in an acousto-optic system (Fig. 1) by a wide-band radio signal of duration τ

$$S(t) = B(t)\cos[\omega_0 t + \psi(t)], \qquad (1)$$

where $\psi(t)$ is a phase function; B(t) is amplitude equal to unity over time τ, is solved by S. M. Rytov's perturbation method [Ref. 2].

The plane light wave

$$E_0(x,z,t) = C_0 \exp\left\{j\left[k(x\sin\varphi + z\cos\varphi) - \Omega t\right]\right\},$$

where $k = \Omega/v_c$ is the wave number of the light; Ω, v_c are the cyclic frequency of the light and its velocity respectively, is incident at angle ϕ to the Oz axis.

Electric field strength E(u, p) satisfies the scalar wave equation

$$\frac{\partial^2}{\partial p^2}E + \beta\frac{\partial^2}{\partial u^2}E + \left[1 + 2\gamma S(u,t)\right]E = 0 \qquad (2)$$

and boundary conditions

$$E(u,-0) = E(u,+0),$$
$$E(u,kl-0) = E(u,kl+0),$$

in the region of acousto-optic interaction $0 \leqslant z \leqslant l$, where $p = kz$; $u = K_0x$; $\beta = (K_0/k)^2$; $K_0 = (\omega_0/v)$ is the wave number of ultrasound on carrier frequency ω_0; v is the velocity of propagation of ultrasound in the acoustic line; $\gamma = (\Delta n/n_0)$ is the relative change in amplitude Δn of the index of refraction of the acoustic line; n_0 is the index of refraction of the unperturbed medium; $S(u, t) = S\left(t - \frac{T}{2} - \frac{u}{K_0 v}\right)$; $T = (L/v)$ is the time sample corresponding to aperture L.

Limiting ourselves to light waves of the zero and first diffraction orders, we will seek the solution of equation (2) in the form

$$E(u,p) = \left[C_0 + \gamma C_1(u,p)\right]\exp\left\{j\left[p\cos\varphi + \frac{u\sin\varphi}{\sqrt{\beta}}\right]\right\}, \qquad (3)$$

where

$$\Phi(u) = \omega_0\left(t - \frac{T}{2}\right) - u + \psi\left(t - \frac{T}{2} - \frac{u}{K_0 v}\right),$$
$$C_1(u,p) = A_{+1}(u,p)\exp\left[j\Phi(u)\right] + A_{-1}(u,p)\exp\left[-j\Phi(u)\right],$$

$A_{\pm1}(u, p)$ are the amplitudes of light waves that describe "plus" and "minus" first diffraction orders.

Since a phase diffraction grating is being used and the angles of diffraction are small, changes of amplitudes $A_{\pm1}$ at distances of the order of a wavelength of ultrasound can be considered small; consequently

$$\left|\frac{\partial}{\partial u}A_{\pm1}(u,p)\right| \ll \left|A_{\pm1}(u,p)\right|$$

and when expression (3) is substituted in (2) we get the following equation:

$$\frac{\partial^2}{\partial p^2}A_{\pm1}(u,p) + 2j\cos\varphi\frac{\partial}{\partial p}A_{\pm1}(u,p) - \beta g_{\pm1}A_{\pm1}(u,p) = -C_0 \qquad (4)$$

with boundary condition

$$A_{\pm1}(u,0) = 0,$$

where

$$g_{\pm 1} = \mp j \frac{\partial^2}{\partial u^2}\psi + \left(\frac{\partial}{\partial u}\psi\right)^2 - \left(\frac{\partial}{\partial u}\psi\right)(2 \mp m) + (1 \mp m), \qquad m = 2\sin\varphi/\sqrt{\beta}. \tag{5}$$

The quantity $g_{\pm 1}$ is complex, and

$$\operatorname{Im} g_{\pm 1} = \mp \frac{1}{\omega_0^2}\left[\frac{\partial^2}{\partial \varepsilon^2}\psi(\varepsilon)\right].$$

where $\frac{\partial^2}{\partial \varepsilon^2}\psi(\varepsilon)$ is the rate of frequency change of signal (1), $\varepsilon = t - \frac{T}{2} - \frac{x}{v}$.

For high-frequency signals $\operatorname{Im} g_{\pm 1}/\operatorname{Re} g_{\pm 1} \ll 1$, and therefore $g_{\pm 1} \approx \operatorname{Re} g_{\pm 1}$. Then disregarding term $\frac{\partial^2}{\partial p^2}A_{\pm 1}$ in equation (4) in virtue of its smallness, and assuming that the angle of incidence ϕ of the plane light wave satisfies the Bragg condition

$$\sin\varphi_0 = \frac{K_0}{2k}, \tag{6}$$

we get a solution $A_{+1}(u, p)$ of equation (4) that takes the form

$$A_{+1}(u, p_\ell) = \left(j C_0 \frac{p_\ell}{2\cos\varphi_0}\right) W_{+1} \exp\left(-j \frac{Q}{2} \operatorname{Re} g_{+10}\right), \tag{7}$$

where

$$W_{+1} = \sin\left(\frac{Q}{2}\operatorname{Re} g_{+10}\right) \Big/ \left(\frac{Q}{2}\operatorname{Re} g_{+10}\right).$$

$Q = (\pi\lambda\ell/\Lambda_0^2)$ is the wave parameter, $\Lambda_0 = (2\pi v/\omega_0)$ is the wavelength of ultrasound on carrier frequency ω_0, $\operatorname{Re} g_{+10} = a(1 + a)$,

$$a = \frac{1}{\omega_0}\left(\frac{\partial}{\partial \varepsilon}\psi(\varepsilon)\right)$$

is the relative frequency change.

Then the light field $E_{+1}(x, \ell, t)$ of the "plus" first diffraction order is described by the expression

$$E_{+1}(x, \ell, t) = \gamma A_{+1}(x, \ell, t) \exp\left[j\, U(x, \ell, t)\right], \tag{8}$$

where

$$U(x, \ell, t) = \omega_0\left(t - \frac{T}{2}\right) - \Omega t - k\ell\cos\varphi_0 + kx\left(\sin\varphi_0 - \frac{K_0}{k}\right) + \psi\left(t - \frac{T}{2} - \frac{x}{v}\right).$$

It should be noted that the function W_{+1} in expressions (7, 8) describes the changes in amplitude of the diffracted light field on frequencies

$$\omega(t) = \omega_0 + \frac{\partial}{\partial t}\psi(t).$$

When the elastic medium of the acoustic line is perturbed by a harmonic signal $\omega(t) = \omega_0$, the amplitude factor W_{+1} is equal to unity and the resultant expressions coincide with those of Ref. 2. The occurrence of the additional factor W_{+1} in solution of the diffraction problem is due to violation of condition (6) on frequencies $\omega(t) \neq \omega_0$.

Computer plots of W_{+1} as a function of relative frequency a at different values of the wave parameter Q are shown on Fig. 2

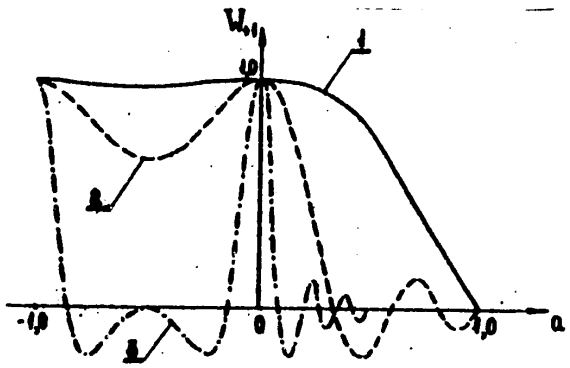

Fig. 2

Curves for W_{+1} as a function of relative frequency and wave parameter:

$1 - Q = \pi$; $2 - Q = 4\pi$; $3 - Q = 16\pi$

It can be seen from Fig. 2 that when light is diffracted by a complex wideband ultrasonic signal, asymmetric distribution of the light field results in the acousto-optical interaction region. With increasing frequency band $\Delta\omega$ of the radio signal and wave parameter Q, there is an increase in amplitude distortions of the diffracted light.

If permissible changes of W_{+1} are assigned, e. g.

$$\frac{\sin\left[\frac{Q}{2}a(1+a)\right]}{\left[\frac{Q}{2}a(1+a)\right]} = \delta,$$

then by finding the value

$$\frac{Q}{2}a(1+a) = \xi,$$

we can readily determine the frequency band

$$\Delta\omega = \omega_0\left[\sqrt{1+\frac{Q_0}{Q}} - 1\right], \qquad (9)$$

where $Q_0 = 8\,\ell$, wherein changes of amplitude do not exceed the value of b.

From expression (9) we determine the wave parameter

$$Q = \frac{Q_0}{\left[\left(\frac{\Delta\omega}{\omega_0}+1\right)^2-1\right]}$$

with respect to the given frequency band, and calculate the optimum length ℓ of acousto-optic interaction:

$$\ell = \frac{\ell_0}{\left[\left(\frac{\Delta\omega}{\omega_0}+1\right)^2-1\right]}, \qquad (10)$$

where $\ell_0 = Q_0\Lambda_0^2/\pi\lambda$.

It should be noted that the resultant expression (10) can be used for calculating the length ℓ of the piezoelectric transducer of an ultrasonic light modulator with respect to given values of the carrier frequency ω_0, frequency bandwidth $\Delta\omega$ of the signals to be processed, and the wavelength of light λ.

Thus the results found in this research enable us to use relatively simple formulas (7, 8) to calculate the diffracted light field $E_{+1}(z, \ell, t)$ in the region of acousto-optical interaction, and the optimum length ℓ (10) of acousto-optical interaction.

The results of this paper may find application both in physical research on the diffraction process and in calculations of acousto-optical devices for processing complex wide-band radio signals.

REFERENCES

1. Raman, C. V., Nagendra Nath, N. S., "The Diffraction of [Light] by [High-] Frequency Sound Waves", PROC. INDIAN ACADEMY OF SCIENCE, Vol 2A, 1935, p 406; Vol 3A, p936, p 25.

2. Rytov, S. M., "Light Diffraction by Ultrasonic Waves", IZVESTIYA AKADEMII NAUK SSSR: SERIYA FIZICHESKAYA, No 2, 1937, p 223.

3. Parygin, V. N., "Light Diffraction by Traveling Acoustic Waves in Isotropic Medium", RADIOTEKHNIKA I ELEKTRONIKA, Vol 19, No 1, 1974, p 38.

4. Bakut, P. A., Chumak, V. G., "Optiko-akusticheskiy korrelyator dlya signala s lineynoy chastotnoy modulyatsiyey" RADIOTEKHNIKA I ELEKTRONIKA, Vol 15, No 9, 1970, p 1916.

5. Karavayev, V. D., Feyzulin, Z. I., "Theoretical Analysis of Acousto-Optic Systems for LFM Radio Signal Compression", TRUDY RADIOTEKHNICHESKOGO INSTITUTA AKADEMII NAUK SSSR", No 5, 1971, p 125.

6. Shulz, M. V., Holland, M. G., Davis, L., "Optical Pulse Compression Using Scattering by Ultrasonic Waves", APPL. PHYS. LETT., Vol 11, No 7, 1967, p 237.

7. Martynov, A. M., Mirer, I. S., "Perturbation Method for Calculating Light Diffraction by Ultrasound", IZVESTIYA VYSSHIKH UCHEBNYKH ZAVEDENIY: RADIOFIZIKA, Vol 18, No 12, 1975, p 1845.

8. Martynov, A. M., "Diffraction of Arbitrary Cylindrical Light Beam by Wide-Band Ultrasonic Signal", RADIOTEKHNIKA I ELEKTRONIKA, Vol 22, No 3, 1977, p 533.

6610
CSO: 8144/0669

- END -